HEAD-TAIL INSTABILITY CAUSED BY ELECTRON CLOUD

E. Perevedentsev*, Budker Institute of Nuclear Physics, Novosibirsk, Russia

Abstract

The strong head-tail instability of a positron or proton bunch may be caused by wakefields arising in the electron cloud present in the beam pipe. These wakefields are known to produce both deflection and tuneshift varying along the bunch. We discuss a model involving this tuneshift as well as the machine chromaticity and transverse feedback.

1 INTRODUCTION

The recent years brought a lot of information concerning the influence of electron cloud on collective dynamics of positron/proton beams, see [1] and references therein. Particularly, observations of the thresholds and growth rates of the transverse beam instabilities at KEKB LER, CERN SPS, and other machines seem to be consistent with the hypothesis of the head-tail instability in a single bunch caused by the cloud wakefields [2], degradation of the effective transverse emittance being a manifestation of this instability.

Our objective in this paper is a detailed characterization of the strong head-tail instability, provided the cloud response is already known. We first consider the properties and parametrization of the electron cloud wake in Sections 2,3. In Section 4.1 we summarize essentials of the standard technique for analysis of single-turn instabilities in a bunched beam, see e. g. [3]. The stability analysis is based on finding the complex tunes of transverse (synchrobetatron) modes from linearized Vlasov equation. We emphasize the role of the machine chromaticity in control of the mode growth rates. The transverse electron cloud wake known from simulations is then used for characterizing the chromaticity-dependent mode tunes in KEKB LER and CERN SPS.

The standard wake and impedance approach can be modified so as to include some specific features of the cloud response. In Section 4.2 we include in our consideration the betatron tune variation along the bunch due to difference in incoherent tuneshifts caused by growth of the cloud density during the bunch passage (pinching of the cloud).

Simulation of the cloud response shows that the cloud pinching results in non-trivial behavior of the transverse dipole wakefield [4, 5], and in Sections 4.3, 4.4 we present the modification of the standard Vlasov eigenvalue problem for the wake function $W_1(z, z')$ which is not reducible to the difference argument $z - z'$.

In Appendices we discuss why the modes with very high order can be disregarded in practical situations. The standard approach can include a simplified model of the transverse bunch-to-bunch feedback, its influence on the beam instability due to electron cloud is discussed in Section 5.

Using the presented techniques, we discuss the typical behavior of the head-tail modes in Section 6, using the parameters of the electron cloud wake for KEKB LER and CERN SPS.

Section 7 is devoted to the estimate of stability based on the coasting-beam limit. And finally, we summarize the results in Conclusion.

2 EQUATIONS OF MOTION

Following the theory of beam-ion or beam-electron interaction [6] we derive one-dimensional equations of motion for our case where the photoelectron cloud is already present prior to arrival of the bunch whose motion is studied.

We write the linear equations for the beam centroid offset $y_b(s, t)$, and electron cloud centroid $y_c(s, t)$ at the machine azimuth s at the time t. Uniform longitudinal density is assumed in both the electron cloud and positron bunch, as well as equal transverse sizes.

$$
\begin{aligned}
\left(\frac{1}{c}\frac{\partial}{\partial t} + \frac{\partial}{\partial s}\right)^2 y_b(s, t) &+ k_0^2\, y_b(s, t) \\
&= g\,(y_c(s, t) - y_b(s, t)), \\
\frac{\partial^2}{\partial t^2} y_c(s, t) &= \omega_c^2\,(y_b(s, t) - y_c(s, t)).
\end{aligned}
$$

Betatron oscillations of the beam are taken in the smooth form with $k_0 = 1/\beta$, β being the vertical amplitude function.

The beam-cloud interaction parameter g can be expressed as

$$
g = \frac{4n_c(\pi\sigma_x\sigma_y)\,e^2}{\gamma mc^2\,\sigma_y(\sigma_x + \sigma_y)} = \frac{4\pi n_c r_e \sigma_x}{\gamma(\sigma_x + \sigma_y)},
$$

n_c is the time-averaged electron cloud density,
σ_y and σ_x are the vertical and horizontal beam sizes,
e is the electron charge,
m is its rest mass,
γ is the beam Lorentz-factor,
c is the speed of light,
r_e is the classical electron radius.

Electrons of the cloud oscillate in the bunch space charge field with the frequency ω_c,

$$
\omega_c^2 = \frac{4N_b\, r_e c^2}{\sqrt{2\pi}\sigma_z \sigma_y(\sigma_x + \sigma_y)},
$$

* perevedent@inp.nsk.su

here N_b is the bunch population and σ_z is its Gaussian length.

We can obtain the equation for the beam centroid alone,

$$\frac{\partial^2}{\partial s^2}y(s,z)+k^2\,y(s,z)=g\frac{\omega_c}{c}\int_0^z dz'\sin\frac{\omega_c}{c}(z-z')y(s,z').$$

With a slowly-varying complex amplitude $A(s,z)$ of the betatron oscillation,

$$y(s,z)=\mathrm{Re}A(s,z)e^{-iks},$$

after averaging out the A^* term on the right-hand side, we have

$$\frac{\partial}{\partial s}A(s,z)=i\frac{g}{2k}\frac{\omega_c}{c}\int_0^z dz'\sin\frac{\omega_c}{c}(z-z')A(s,z').$$

Thus the problem is reduced to the beam breakup with an oscillating transverse dipole wake function $W(z-z')$,

$$W(z-z')\propto g\frac{\omega_c\sigma_z}{cN_b}\sin\frac{\omega_c}{c}(z-z').$$

3 DECOHERENCE AND PARAMETRIZATION OF THE WAKE FUNCTION

Non-uniformity of the positron bunch density leads to the frequency spread of the photoelectron oscillation and results in decoherence of the cloud response. A simple estimate can be done by averaging the wake with a weight function $f(x)$ which implies e. g. horizontal non-uniformity of the bunch distribution affecting the vertical wake function:

$$W(\omega_c,z)\rightarrow\int W(\omega_c(x),z)f(x)dx.$$

If we take a Gaussian distribution of the beam density,

$$f(x)=\sqrt{\frac{2}{\pi}}e^{-x^2/2},$$

then

$$\omega_c(x)=\omega_0 e^{-x^2/4}.$$

Hence we obtain the wake with the account of decoherence,

$$\tilde{W}(z)=g\frac{\omega_0 l}{c}\int_0^\infty\sin\left(\frac{\omega_0 z}{c}e^{-x^2/4}\right)\sqrt{\frac{2}{\pi}}e^{-3x^2/4}dx.$$

The result can be expressed in terms of the Struve function and can be fitted either by the Bessel function $J_1(\omega_0 z/c)$ for large z, or by the broad-band resonator wake,

$$W_1(z) = \frac{cR_S\omega_R}{Q\bar{\omega}}e^{-\alpha z/c}\sin\frac{\bar{\omega}z}{c},\ (z>0),$$
$$\alpha = \frac{\omega_R}{2Q},\qquad \bar{\omega}=\sqrt{\omega_R^2-\alpha^2}.$$

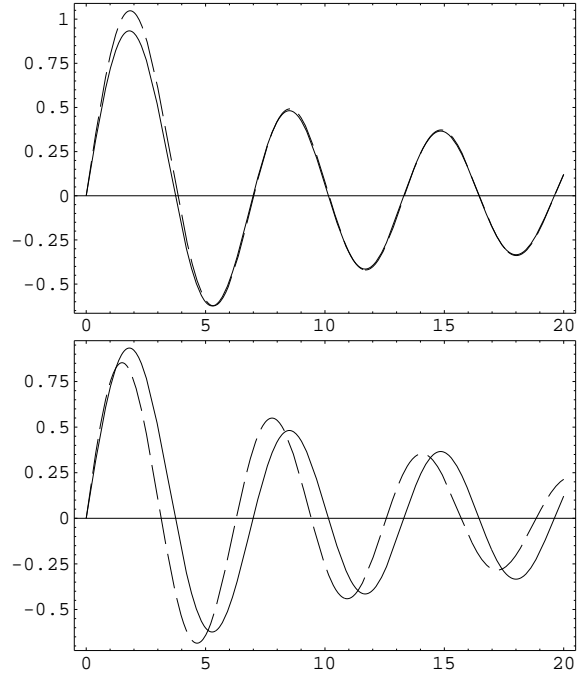Figure 1 shows the comparison of these fits with actual $\tilde{W}(z)$.

Figure 1: The decoherence wake $\tilde{W}(z)$ (solid line) and the fitting function (dashed line). Top: fit by the Bessel function $J_1(\omega_0 z/c)$; bottom: fit by the broad-band resonator with $\overline{\omega}=\omega_0$.

The corresponding transverse impedance is sampled by the long bunch spectrum in the low-frequency range ($\omega_R\sigma_z/c\sim 3$ at KEKB LER),

$$Z_1=\frac{cR_S/Q}{\dfrac{\omega}{Q}+i\left(\omega_R-\dfrac{\omega^2}{\omega_R}\right)}\approx\frac{cR_S}{Q\omega_R}\left(\frac{\omega}{Q\omega_R}-i\right).$$

The broad-band resonator parameters relevant to the KEKB LER and the SPS (see Table 1 for the parameter lists) are determined from the simulations of the wake function [4, 5], and listed in Tables 2,3.

4 STRONG HEAD-TAIL INSTABILITY

In contrast to the beam break-up problem in a linac, the dynamics in a circular machine is strongly affected by the synchrotron oscillations. The electron cloud effect on coherent motion of the single bunch can be modelled by the strong head-tail instability [2]. This will be the framework of the stability analysis in the following section.

4.1 Standard Case, the Transverse Wake Function in the Form $W(z-z')$[1]

Notation:
N_b is the number of positrons in a bunch,

---

[1]In this subsection we closely follow the derivation presented in Chapter VI of A.W. Chao, *Physics of Collective Instabilities in High Energy Accelerators* (J. Wiley, New York,1993), and refer to the equations therein using the format "Eq. (6.xxx)" in the following part of the paper.

Table 1: Basic parameters of the KEKB LER and CERN SPS

variable	KEKB-LER	SPS
particle type	e^+	p
circumference	3016 m	6900 m
beam energy	3.5 GeV	26 GeV
bunch population	3.3×10^{10}	$1. \times 10^{11}$
bunch spacing	8 ns	—
rms beam sizes	0.42 mm	3 mm
	0.06 mm	2.3 mm
bunch length	5 mm	30 cm
rms energy spread	0.0007	0.002
slippage factor	1.8×10^{-4}	5.8×10^{-4}
chromaticity	4/8	0/10
synchrotron tune	0.015	0.0046
betatron tune	$\sim$46.	26.7
average beta function	15 m	40 m

Table 2: Analytically determined parameters for wake force induced by electron cloud using the resonator approximation. R/Q in units of Ω can be obtained by $cR_S/Q \times 30$. cR_S/Q and ω_b^2, which linearly depend on ρ, are evaluated for $\rho_c = 10^{12}$ m^{-3}.

	KEKB-LER		CERN-SPS
	x	y	y
$\omega_c[\mathrm{s}^{-1}]$	6.4×10^{10}	1.70×10^{11}	1.5×10^9
$\omega_b[\mathrm{s}^{-1}]$	1.7×10^5	4.5×10^5	1.4×10^5
$cR_S/Q[\mathrm{m}^{-2}]$	1.5×10^5	2.9×10^6	8.3×10^5

Table 3: Simulated parameters for the wake field induced by an electron cloud of density $\rho_e = 10^{12}$ m^{-3}, as obtained by fitting to the resonator model.

	KEKB-LER		SPS
	x	y	y
$\omega_R[\mathrm{s}^{-1}]$	8.7×10^{10}	2.2×10^{11}	1.5×10^9
Q	2.7	6.3	4.9
$cR_S/Q[\mathrm{m}^{-2}]$	2.9×10^6	8.3×10^6	3.2×10^6

$\rho_{x(y)}(s, z')$ is the horizontal (vertical) dipole moment of particles at z',

η is the slippage factor,

δ is the relative momentum deviation,

$\omega_{\beta,x(y)} = c/\beta_{x(y)}$ is the horizontal (vertical) angular betatron frequency in the smooth approximation,

$\xi = \dfrac{E}{\omega_{\beta,x(y)}} \dfrac{\partial \omega_{\beta,x(y)}}{\partial E}$ is the chromaticity,

ω_s is the angular synchrotron frequency.

The beam distribution function can be split into the un-perturbed term and a single-frequency perturbation,

$$\Psi = \Psi_0 + \Psi_1 e^{-i\Omega s/c},$$

and Ψ_0 is expressed via functions of the unperturbed invariants of motion for each degree of freedom,

$$\Psi_0 = \psi_0(q)\varphi_0(r),$$

where

$$
\begin{aligned}
r &= \sqrt{z^2 + \left(\frac{\eta c}{\omega_s}\delta\right)^2}, \\
z &= r\cos\phi, \quad \delta = \frac{\omega_s r}{\eta c}\sin\phi, \\
q &= \sqrt{y^2 + \left(\frac{c}{\omega_{\beta,y}}p_y\right)^2}, \\
y &= q\cos\theta, \quad p_y = -\frac{q\omega_{\beta,y}}{c}\sin\theta.
\end{aligned}
$$

The Vlasov equation is linearized for a small perturbation of the distribution function, $\Psi_1(q, \theta, r, \phi)$:

$$
\left[i\frac{\Omega}{c}\Psi_1 - \frac{\omega_\beta}{c}(1 + \xi\delta)\frac{\partial\Psi_1}{\partial\theta} - \frac{\omega_s}{c}\frac{\partial\Psi_1}{\partial\phi}\right]e^{-i\Omega s/c}
$$
$$
+ \frac{c^2}{\omega_\beta}\frac{\partial\Psi_0}{\partial q}\sin\theta F(s, z) = 0, \qquad (1)
$$

where the action of transverse dipole wakefield $W_1(z - z')$ is represented by the force

$$
F(s, z) = -\frac{N_b r_e}{\gamma}\int W_y(z - z')\rho_{y,1}(s, z')dz', \qquad (2)
$$

and $\rho_{y,1}(s, z')$ is the vertical dipole moment of particles at z' for the perturbed distribution Ψ_1.

In the dipole approximation, the solution should be a function of q and θ in the form which follows from Eqs. (6.168–169,175),

$$
\Psi_1 \propto \frac{\partial\Psi_0}{\partial q}e^{i\theta}K(r)\sum_{lk}a_{lk}f_{lk}(r)e^{il\phi}e^{i\chi(\phi)}, \qquad (3)
$$

where $\chi(\phi)$ is the chromatic phase, $\chi(\phi) = \xi\omega_\beta r\cos\phi/c\eta$, and $f_{lk}(r)$ form a set of orthogonal functions which characterize radial modes and satisfy the normalization

$$
\int_0^\infty K(r)f_{lk}(r)f_{lk'}(r)rdr = \delta_{kk'}, \qquad (4)
$$

$K(r)$ being the weight function of radial modes. This weight function is related to the unperturbed longitudinal distribution $\varphi_0(r)$:

$$
K(r) = \frac{\omega_s}{\eta c}\varphi_0(r). \qquad (5)
$$

By using the expansion Eq. (3) in Eq. (1), replacing $\sin\theta \to e^{i\theta}/2i$ in the smooth approximation, rewriting the force Eq. (2) in the frequency domain via the impedance,

and substituting the Fourier transform of the dipole moment distribution from Eq. (6.75), the problem is reduced to a linear equation set, and Ω is to be found from the corresponding eigenvalue problem,

$$\left(\frac{\Omega - \omega_\beta}{\omega_s}\right) a_{lk} = (l\delta_{ll'}\delta_{kk'} + M_{lk,l'k'}) a_{l'k'}. \quad (6)$$

The matrix M is expressed by

$$
\begin{aligned}
M_{lk,l'k'} &= -i\frac{N_b r_e c}{2\gamma T_0 \omega_\beta \omega_s} i^{l-l'} \quad (7)\\
&\times \int_{-\infty}^{\infty} Z_1(\omega) g_{lk}(\omega - \omega_\xi) g_{l'k'}(\omega - \omega_\xi)\, d\omega
\end{aligned}
$$

where we introduced

$$g_{lk}(\omega) = \int_0^{\infty} r\,dr\,K(r) f_{lk}(r) J_l\left(\frac{\omega}{c}r\right), \quad (8)$$

and $\omega_\xi = \xi\omega_\beta/\eta$ is the chromatic frequency.

The wake force enters via its impedance representation,

$$Z_1(\omega) = i\int_{-\infty}^{\infty} \frac{dz}{c} e^{-i\omega z/c} W_1(z). \quad (9)$$

If we take the broad-band resonator impedance model, then for given shunt impedance R_S, quality factor Q, and resonator frequency ω_R, the impedance is expressed as

$$Z_1(\omega) = \frac{c}{\omega} \frac{R_S}{1 + iQ\left(\frac{\omega_R}{\omega} - \frac{\omega}{\omega_R}\right)}. \quad (10)$$

For a Gaussian distribution in the longitudinal phase space, the unperturbed distribution function and the weight function can be written as

$$\varphi_0(r) = \frac{\eta c e^{-r^2/2\sigma^2}}{2\pi\sigma^2\omega_s}, \quad K(r) = \frac{e^{-r^2/2\sigma^2}}{2\pi\sigma^2}. \quad (11)$$

The orthonormal radial functions are the generalized Laguerre polynomials

$$f_{lk}(r) = \sqrt{\frac{2\pi k!}{(|l|+k)!}} \left(\frac{r}{\sqrt{2}\sigma}\right)^{|l|} L_k^{|l|}\left(\frac{r^2}{2\sigma^2}\right), \quad (12)$$

then from Eq. (8),

$$
\begin{aligned}
g_{lk}(\omega) &= \frac{\varepsilon(l)}{\sqrt{2\pi k!(|l|+k)!}} \left(\frac{\omega\sigma}{\sqrt{2}c}\right)^{|l|+2k} e^{-\omega^2\sigma^2/2c^2},\\
\varepsilon(l) &= \begin{cases} 1, & l \geq 0;\\ (-1)^l, & l < 0. \end{cases} \quad (13)
\end{aligned}
$$

This corresponds to the Hermite modes of the dipole moment,

$$\rho_y(z) \propto e^{-z^2/2\sigma^2} H_{|l|+2k}\left(\frac{z}{\sqrt{2}\sigma}\right). \quad (14)$$

We consider here the azimuthal mode coupling only for three lowest radial modes ($k = 0, 1, 2$). The coupling matrix consists of 9 blocks,

$$M = \begin{pmatrix} l\delta_{ll'} + M_{l0,l'0} & M_{l0,l'1} & M_{l0,l'2}\\ M_{l1,l'0} & l\delta_{ll'} + M_{l1,l'1} & M_{l1,l'2}\\ M_{l2,l'0} & M_{l2,l'1} & l\delta_{ll'} + M_{l2,l'2} \end{pmatrix}, \quad (15)$$

$$
\begin{aligned}
M_{lk,l'k'} &= -i\frac{N_b r_e c}{4\pi\gamma T_0 \omega_\beta \omega_s} \frac{i^{l-l'}\varepsilon(l)\varepsilon(l')}{\sqrt{k!(|l|+k)!k'!(|l'|+k')!}}\\
&\times \int_{-\infty}^{\infty} Z_1(\omega + \omega_\xi) e^{-\omega^2\sigma^2/c^2} \left(\frac{\omega\sigma}{\sqrt{2}c}\right)^{|l|+|l'|+2(k+k')} d\omega.
\end{aligned}
$$

Before computing, the integration variable ω should be changed to the dimensionless $w = \omega\sigma/c$, and accordingly we introduce

$$w_R = \omega_R\sigma/c, \quad \chi = \omega_\xi\sigma/c = \nu_\beta\xi\frac{\sigma_E/E}{\nu_S},$$

$$\frac{c}{\sigma}Z_1(\omega) = \frac{cR_S/Q}{w/Q + i(w_R - w^2/w_R)}. \quad (16)$$

Here χ is the effective value of chromatic phase for a Gaussian bunch, and the impedance is substituted from the broad-band resonator model, Eq. (10). Then we rewrite the mode coupling matrix as

$$
\begin{aligned}
M_{lk,l'k'} &= -i\frac{N_b r_e c(cR_S/Q)}{4\pi\gamma T_0 \omega_\beta \omega_s} \frac{i^{l-l'}\varepsilon(l)\varepsilon(l')}{\sqrt{k!(|l|+k)!k'!(|l'|+k')!}}\\
&\times \int_{-\infty}^{\infty} \frac{(w/\sqrt{2})^{|l|+|l'|+2(k+k')} e^{-w^2} dw}{(w+\chi)/Q + i(w_R - (w+\chi)^2/w_R)}. \quad (17)
\end{aligned}
$$

The tune of each mode $(\Omega - \omega_\beta)/\omega_s$ is obtained by solving the eigenvalue problem, Eq. (6), for matrix $l\delta_{ll'}\delta_{kk'} + M_{lk,l'k'}$. At $N_b \to 0$ the mode frequency $\Omega = \omega_\beta + l\omega_s$ corresponds to the lth synchrobetatron sideband. The matrix has infinite dimension because of $-\infty < l < \infty$.

For most cases considered below we can truncate the matrix at $-5 \leq l \leq 4$, and calculate the eigenvalues numerically. To check-up the convergency, we compared the eigenvalues with those of the truncation at $-9 \leq l \leq 6$.

4.2 Betatron Tune Variation Along the Bunch

The transverse fields of the positron/proton bunch cause variation of the effective transverse size of electron cloud over the bunch passage. The variable density of the cloud results in different incoherent tuneshifts along the bunch. Simulation shows that in some cases we can only consider the linear part of the tune variation along the bunch [5].

Let us modify the standard analysis of Section 4.1 to include this effect. Now, in addition to the chromaticity effect, we have to introduce the betatron frequency variation term $\zeta z/\sigma$, then

$$\omega_\beta(\delta, z) = \omega_\beta(1 + \xi\delta + \zeta z/\sigma)$$

and the transverse dipole perturbation Ψ_1 in the Vlasov equation (1) should be decomposed as

$$\Psi_1 \propto \frac{\partial \Psi_0}{\partial q} e^{i\theta} K(r) \sum_{lk} a_{lk} f_{lk}(r) e^{il\phi} e^{i\chi(\phi) - i\Delta(\phi)}, \quad (18)$$

where besides the chromatic phase,

$$\chi(\phi) = \xi \omega_\beta r \cos \phi / c\eta = \omega_\xi r \cos \phi / c, \ \omega_\xi = \xi \omega_\beta / c\eta,$$

we introduced

$$\Delta(\phi) = \zeta \omega_\beta r \sin \phi / \sigma \omega_s = \omega_\zeta r \sin \phi / c, \ \omega_\zeta = \zeta \omega_\beta c / \sigma \omega_s.$$

This will modify the Bessel function argument in Eqs. (6.74,75) and henceforth,

$$\int_0^{2\pi} \frac{d\phi}{2\pi} \exp[-il\phi + i\omega \frac{z}{c} - i(\omega_\xi \cos \phi - \omega_\zeta \sin \phi) \frac{r}{c}]$$
$$= i^l e^{-il\phi_0} J_l(\frac{r}{c} \sqrt{(\omega - \omega_\xi)^2 + \omega_\zeta^2}),$$

where

$$\phi_0 = \arg(\omega - \omega_\xi + i\omega_\zeta).$$

As a consequence, we should modify the mode spectra in Eq. (7) using Eq. (8),

$$g_{lk}(\sqrt{(\omega - \omega_\xi)^2 + \omega_\zeta^2}) = e^{-il\phi_0} \int_0^\infty r\, dr\, K(r) f_{lk}(r)$$
$$\times J_l(\frac{r}{c} \sqrt{(\omega - \omega_\xi)^2 + \omega_\zeta^2}),$$

and thus the formalism for the longitudinal tune variation is ready.

For the Gaussian bunch we only have to replace the arguments of $g_{lk}(\omega)$ in Eq. (13),

$$
\begin{aligned}
g_{lk}(\omega - \omega_\xi, \omega_\zeta) &= \frac{\varepsilon(l) e^{-((\omega - \omega_\xi)^2 + \omega_\zeta^2)\sigma^2/2c^2}}{\sqrt{2\pi k!(|l| + k)!}} \\
&\times \left(\frac{\sigma(\omega - \omega_\xi - i\omega_\zeta)}{\sqrt{2}c} \right)^{|l|} \\
&\times \left(\frac{\sigma^2((\omega - \omega_\xi)^2 + \omega_\zeta^2)}{2c^2} \right)^k, \\
\varepsilon(l) &= \left\{ \begin{array}{ll} 1, & l \geq 0; \\ (-1)^l, & l < 0. \end{array} \right.
\end{aligned}
$$

The final form of the coupling matrix for the Gaussian bunch and broad-band resonator impedance now is

$$M_{lk,l'k'} = -i \frac{N_b r_e c (cR_S/Q)}{4\pi \gamma T_0 \omega_\beta \omega_s} \frac{i^{l-l'} \varepsilon(l) \varepsilon(l')}{\sqrt{k!(|l|+k)! k'!(|l'|+k')!}}$$
$$\times \int_{-\infty}^\infty \frac{A(w) dw}{(w + \chi)/Q + i(w_R - (w + \chi)^2/w_R)}, \quad (19)$$

$$A(w) = \frac{(w - i\Delta)^{|l|}(w + i\Delta)^{|l'|}(w^2 + \Delta^2)^{k+k'}}{2^{k+k'+(|l|+|l'|)/2}} e^{-w^2 - \Delta^2}.$$

The eigenvalues do not depend on the sign of Δ.

With the same SPS parameters as used in Figs. 6,7, we can see in Figs. 15,16 the stabilizing effect of the tune variation at $\Delta \geq 1$, as predicted in [7]. The positive chromaticity effect remains, see Fig. 17.

4.3 General Case, the Transverse Wake Function in the Form $W(z, z')$

For more general situations, e. g., for the electron cloud response to dipole perturbations, translation invariance in z does not hold, and the wake function cannot be reduced to the form $W(z - z')$. We now trace the differences in the linearized Vlasov formalism resulting from the general form of the wake, $W_1(z, z')$. This function must vanish for $z > z'$.

First we introduce its full Fourier transform $\hat{Z}_1(\omega, \omega')$ and call it *a generalized impedance*,

$$W_1(z, z') = \int \int \frac{d\omega}{2\pi} \frac{d\omega'}{2\pi} \frac{1}{i} \hat{Z}_1(\omega, \omega') e^{i(\omega z - \omega' z')/c}. \quad (20)$$

The particular case where $\hat{Z}_1(\omega, \omega') = 2\pi \delta(\omega - \omega') Z(\omega)$ corresponds to the conventional wake $W_1(z - z')$.

Substituting Eq. (20) into Eq. (2), we find the transverse force

$$F(s, z) = -\frac{N_b r_e}{\gamma} e^{-i\Omega s/c} \int W_1(z, z') \rho_1(z') dz'$$
$$= \frac{N_b r_e}{\gamma} e^{-i\Omega s/c} \int \frac{d\omega}{2\pi} e^{i\omega z} \int \frac{d\omega'}{2\pi} \tilde{\rho}_1(\omega') \hat{Z}_1(\omega, \omega'), \quad (21)$$

where

$$\tilde{\rho}_1(\omega) = \int dz\, e^{-i\omega z/c} \rho_1(z) \quad (22)$$

is the Fourier transform of the beam dipole moment distribution $\rho_1(z)$. Using a derivation shown in Eq. (6.75), we arrive at the result of Eq. (6.178),

$$\tilde{\rho}_1(\omega') = 2\pi \frac{\omega_s}{c\eta} \sum_{l,k} \int_0^\infty r\, dr\, K(r)$$
$$\times a_{lk} f_{lk} i^{-l} J_l((\omega' - \omega_\xi) r/c). \quad (23)$$

We put this expression in Eq. (1) transformed appropriately (cf. the derivation of Eq. (6.177)),

$$i \left(\frac{\Omega - \omega_\beta}{\omega_s} - l \right) K(r) \sum_{k'} a_{lk'} f_{lk'} = \frac{N_b r_e c i^l \varphi_0(r)}{4\pi \gamma \omega_\beta \omega_s T_0}$$
$$\times \int \frac{d\omega}{2\pi} J_l((\omega - \omega_\xi) r/c) \int \frac{d\omega'}{2\pi} \tilde{\rho}_1(\omega') \hat{Z}_1(\omega, \omega'), \quad (24)$$

and relating the weight function $K(r)$ to the unperturbed distribution $\varphi_0(r)$, Eq. (5), we only need to use the orthonormality condition Eq. (4) to reduce the integral equation Eq. (24) to a linear equation set in the basis of mode functions f_{lk},

$$\left(\frac{\Omega - \omega_\beta}{\omega_s} - l \right) a_{lk} = -\frac{N_b r_e c}{2\gamma \omega_\beta \omega_s T_0} \sum_{l'k'} \hat{M}_{lk,l'k'} a_{l'k'}, \quad (25)$$

where the general mode coupling matrix $\hat{M}_{lk,l'k'}$ is expressed via the generalized impedance,

$$\hat{M}_{lk,l'k'} = -i \frac{N_b r_e c i^{l-l'}}{4\pi \gamma \omega_\beta \omega_s T_0}$$

$$\times \int\int d\omega d\omega' g_{lk}(\omega - \omega_\xi) g_{l'k'}(\omega' - \omega_\xi)\hat{Z}_1(\omega,\omega'), \quad (26)$$

while the mode spectrum $g_{lk}(\omega)$ is given by Eq. (8), as for the standard case.

Going to the time domain, we introduce the dipole moment distributions corresponding to the mode spectra,

$$\tilde{g}_{lk}(z) = \int \frac{d\omega}{2\pi c} g_{lk}(\omega)e^{i\omega z/c}, \quad \tilde{g}_{lk}(-z) = \tilde{g}_{lk}^*(z), \quad (27)$$

and rewrite the double integral, in Eq. (26),

$$\hat{M}_{lk,l'k'} = \frac{\pi N_b r_e c i^{l-l'}}{\gamma \omega_\beta \omega_s T_0} \int_{-\infty}^{\infty} dz\, \tilde{g}_{lk}^*(z)$$
$$\times \int_z^{\infty} dz'\, \tilde{g}_{l'k'}(z')W(z,z')e^{-i\omega_\xi(z-z')} \quad (28)$$

It is easy see that at vanishing chromaticity, $\omega_\xi = 0$, all the matrix elements are real numbers.

This time-domain form may give an advantage in computation of the mode coupling matrix.

4.4 Gaussian Bunch

For the radial head-tail modes of the Gaussian bunch, we use Eqs. (11-13) to write the final form of the mode coupling matrix,

$$\hat{M}_{lk,l'k'} = -i\frac{N_b r_e c}{8\pi^2 \gamma T_0 \omega_\beta \omega_s} \frac{i^{l-l'}\varepsilon(l)\varepsilon(l')}{\sqrt{k!(|l|+k)!k'!(|l'|+k')!}}$$
$$\times \int_{-\infty}^{\infty}\int_{-\infty}^{\infty} d\omega d\omega' \hat{Z}_1(\omega + \omega_\xi, \omega' + \omega_\xi)$$
$$\times \left(\frac{\omega\sigma}{\sqrt{2}c}\right)^{|l|+2k}\left(\frac{\omega'\sigma}{\sqrt{2}c}\right)^{|l'|+2k'} e^{-(\omega^2+\omega'^2)\sigma^2/2c^2}. \quad (29)$$

To obtain the time-domain form, we transform the mode spectra, Eq. (13), and get

$$\tilde{g}_{lk}(z) = \frac{\Gamma(k + \frac{1+|l|}{2})}{2\pi\sigma\sqrt{\pi k!(|l|+k)!}}\,{}_1F_1(k + \frac{1+|l|}{2}, \frac{1}{2}; -\frac{z^2}{2\sigma^2}), \quad (30)$$

for even l, and

$$\tilde{g}_{lk}(z) = i\,\mathrm{sign}l\frac{\Gamma(k+1+\frac{|l|}{2})}{2\pi\sigma\sqrt{\pi k!(|l|+k)!}}\left(\frac{z}{\sqrt{2}\sigma}\right)$$
$$\times {}_1F_1(k+1+\frac{|l|}{2}, \frac{3}{2}; -\frac{z^2}{2\sigma^2}), \quad (31)$$

for odd l. Of course, the hypergeometric function can be reduced to the "oscillator wave functions" expressed via the Hermite polynomials, see Eq. (14). However, for higher-order modes the above form is more efficient in computation. For $z \geq \sigma\sqrt{|l| + 2k}$ these functions have a Gaussian cut-off, and thus the infinite integration range in Eq. (28) is not a serious problem. Finally we have to substitute Eqs. (30,31) into Eq. (28) in order to evaluate the general mode coupling matrix for the Gaussian bunch.

5 A SIMPLE MODEL OF TRANSVERSE FEEDBACK

A bunch-to-bunch feedback integrates the dipole moment over the total bunch length ($\sigma_z = 5$mm at KEKB!) and applies its proportional kick after one turn, with a tunable gain and phase shift. The feedback kicker pulse is practically constant over this bunch length. At KEKB $2\pi\nu_s \ll 1$, thus the one-turn delay may not cause a problem like in LEP machine.

Assuming a perfectly linear (no gain saturation) and noiseless feedback hardware, we can describe its action by an equivalent transverse impedance,

$$Z_{FB} = -ig_{FB}e^{i\phi_{FB}}\delta(\omega)$$

where g_{FB} and ϕ_{FB} are the feedback gain and phase.

The feedback phase parameter can be tuned to purely resistive, $\phi_{FB} = \pi/2$, or purely reactive, $\phi_{FB} = 0, \pi$, or mixed mode.

At zero chromaticity, the feedback only acts upon the $l = 0$ mode; at positive chromaticity, higher-order synchrobetatron modes are also influenced.

6 TYPICAL BEHAVIOR OF THE MODE TUNES

The eigenvalues of truncated M, Eq. (17) (i. e., tunes of each mode) are computed as functions of cR_S/Q at fixed bunch intensity, using ω_R and Q from the wake simulation for KEKB LER and CERN SPS [4, 5].

The following figures show the computed mode tunes vs R_S/Q or the cloud density ρ_c, since R_S/Q is linearly related with it.

The positive slope of all the mode tunes resulting from incoherent effect of the electron cloud (single-particle focusing by the cloud) is equal in all the modes; it is ignored in the following figures.

The parameters of the transverse dipole wake from the electron cloud correspond to large values of the wake oscillation parameter $p = \omega_R\sigma_z/c$. For KEKB LER $p = 3$, for CERN SPS $p = 1.5$. So, we are working with the case of "long" bunch, the beam spectrum samples the low-frequency part of the cloud impedance. An important consequence is that the positive chromaticity results in damping of all the lower-order head-tail modes up to orders $|l| + 2k \sim p^2$, at least for small bunch intensities, $\Delta\nu_{\mathrm{coh}} \ll \nu_s$.

The above statement does not contradict with the vanishing sum of all decrements, see Appendix A. The damping of a dozen lower-order modes is balanced by the weak anti-damping of a great many of higher-order modes. However, their weak instability is not important because of stabilization by the incoherent tune spread of any nature, or by quantum fluctuations in electron/positron machines, see Appendix B.

At high intensity the mode coupling becomes important, although for the long-bunch case the diagonal elements in

the mode coupling matrix tend to dominate. With sufficiently high chromaticities, $\chi \sim 2$, all the lower-order modes included in truncation become stable, i. e. the high positive chromaticity can significantly enhance the TMCI threshold for "long" bunches.

Figures 2,3 show the effect of positive chromaticity for the parameters of KEKB LER. With higher values of Q, see Figs. 4,5, the chromaticity effect becomes more pronounced. The instability thresholds with $Q = 1$, Figs. 2,3, are in reasonable agreement with observations of the positron beam blowup at KEKB LER [8].

The same effect is shown in Figs. 6,7 with the parameters relevant to the CERN SPS. The chromaticity dependence shown is consistent with the electron cloud instability simulation for this machine [9].

Now return to the KEKB LER. The transverse feedback is not very efficient against rather high increments of the TMCI at zero chromaticity, Fig. 8. However, the feedback tuned resistive, and in combination with the moderate positive chromaticity, can seriously raise the threshold, Fig. 9. The same enhancement from the reactive feedback alone, Figs. 10,11, leads to a conclusion that the parameters of the bunch-to-bunch feedback, including its phase, can be optimized with respect not only to the residual dipole oscillation, but also to the beam blowup believed to be caused by the electron cloud. And in combination with the chromaticity, Fig. 12, the effect of the feedback phase is stronger.

Dependence of the instability threshold on the bunch current with different filling patterns at KEKB LER is shown in Figs. 13,14. Here variation of the bunch current means proportional variation of the cloud density plus the square-root scaling of the wake oscillation frequency ω_R.

For the parameters of CERN SPS, Figs. 15,16 show the mode coupling dependence at 6 different gradients of the linear tune variation along the bunch, the tune variation of 1 means that the incoherent tune shift varies from Q_s to $-Q_s$ over $\pm\sigma_z$. The graphs demonstrate the stabilizing effect from the longitudinal variation of incoherent betatron tune, cf. [7]. Fig. 17 presents the effect of the positive chromaticity at fixed tune variation parameter.

7 MODE STABILITY IN THE COASTING BEAM LIMIT

Using the coasting-beam limit, $\omega_R \sigma_z / c \gg 1$, for estimation of the bunched-beam stability, one usually takes the maximum of $\mathrm{Re}\,Z_1$ to be sure that *all the modes* are stable. For the BBR $\omega_{max} \approx \omega_R$, this means $\mathrm{Re}\,Z_1(\omega_R)$.

However, for our case with low mode numbers, $l \sim 1$, and $lc/\sigma_z \ll \omega_R$, this will yield too strong a condition (sufficient, but not necessary).

Let us take the coasting-beam limit condition for stability in its *full form*, see Eq. (6.263) in [3]:

$$-\frac{N}{cT_0}\frac{r_e c^2}{2\gamma T_0 \omega_\beta}\mathrm{Re}\,Z_1(n\bar\omega_0 + \omega_\beta) < \Delta\delta| - n\bar\omega_0\eta + \xi\omega_\beta|,$$

with the linear density corresponding to that in the bunch,

$$\frac{N_b}{\sqrt{2\pi}\sigma_z} \leftarrow \frac{N}{cT_0},$$

and $\Delta\delta$ corresponding to σ_E/E for Gaussian bunches.

Relating this coasting beam situation to the bunched beam parameters, we should also replace

$$
\begin{aligned}
n\bar\omega_0 &\rightarrow \omega \text{ of the mode}\\
\xi\omega_\beta/\eta &\rightarrow \omega_\xi, \text{ the chromatic frequency}\\
c\eta\Delta\delta/\omega_s &\rightarrow \sigma_z, \text{ the bunch length}
\end{aligned}
$$

For the higher-order modes the accurate treatment by the TMC theory shows stability.

For the lower-order modes, $l \sim 1 - 2$, we take

$$\omega \simeq -\frac{c}{\sigma_z}l \; (\ll \omega_R)$$

and approximate the impedance

$$\mathrm{Re}\,Z_1 \approx \frac{cR_S}{Q}\frac{\omega}{Q\omega_R^2}.$$

Then, neglecting $\omega_\beta \ll \omega$, we obtain the stability condition for the lth mode

$$\frac{Nr_e c^2}{2\gamma T_0^2 \omega_\beta \omega_s \sigma_z}\frac{cR_S}{Q}\frac{1}{Q\omega_R^2} < \left|1 + \frac{\omega_\xi \sigma_z}{cl}\right| = |1 + \chi/l|\,,$$

where χ is the chromatic phase. Note that $\omega_R^2 \propto N_b/\sigma_z \propto N$, $cR_S/Q \propto \rho_c$, and $\omega_s \sigma_z \propto \eta$.

Hence, we come to the scaling of the threshold level of the electron cloud density

$$\rho_{c,\mathrm{th}} \propto \eta\,Q\,|1 + \chi/l|, \text{ for } l \sim 1 - 2.$$

For the case $\omega \approx -\omega_R$, we approximate

$$\mathrm{Re}\,Z_1 \approx \frac{cR_S}{Q}\frac{Q}{\omega_R},$$

and arrive at somewhat different stability condition,

$$\frac{Nr_e c^2}{2\gamma T_0^2 \omega_\beta \omega_s \sigma_z}\frac{cR_S}{Q}\frac{Q}{\omega_R^2} < |1 + \omega_\xi/\omega_R|\,,$$

whence the threshold scaling is

$$\rho_{c,\mathrm{th}} \propto \frac{\eta}{Q}|1 + \chi\frac{c}{\omega_R\sigma_z}|, \text{ for } l \sim \omega_R\sigma_z/c,$$

i. e. the mode number is replaced with the wake oscillation parameter. In the saturation condition, $\rho_{c,\mathrm{th}} \propto N_{b,\mathrm{th}}/L_{\mathrm{sep}}$.

For the opposite situation, $\omega_R\sigma_z/c \ll 1$, from the single-bunch interaction parameter $Z_1 N_b/\sigma_z$, with $Z_1 \propto \rho_c$, we find a different scaling of the instability threshold,

$$Z_1 N_b/\sigma_z \propto N_b^2/\sigma_z L_{\mathrm{sep}}.$$

8 CONCLUSION

The paper presents analytical tools for studies of strong head-tail instability caused by electron cloud, including the machine chromaticity. The standard multi-mode eigenvalue analysis of the transverse mode coupling is extended by including into consideration the specific properties of the cloud response caused by its pinching, Section 4.

On the basis of this study we come to a conclusion on very important role of the high positive chromaticity, the most appropriate measure of its stabilizing effect being the respective chromatic phase χ. In different parameter sets considered in Section 6 we always obtained stabilization at $\chi \sim 2$ radian. Smaller values of the chromaticity were nevertheless efficient in combination with the transverse bunch-to-bunch feedback system.

Although it is difficult to take into full account analytically such a complex phenomenon as the electron cloud, the analytical effort applied to simplified dynamical models may provide some insight and help in better understanding the results of simulation studies of the beam dynamics under the influence of the electron cloud.

9 ACKNOWLEDGEMENTS

10 REFERENCES

[1] F. Zimmermann, "The Electron CLoud Instability: Summary of Measurements and Understanding", presented at PAC'2001, Chicago, 2001, CERN-SL-2001-035(AP), (2001).

[2] K. Ohmi and F. Zimmermann, Phys. Rev. Lett. **85**, 3821 (2000).

[3] A.W. Chao, *Physics of Collective Instabilities in High Energy Accelerators* (J. Wiley, New York,1993).

[4] K. Ohmi et al., Phys. Rev. E **65** 016502 (2001).

[5] F. Zimmermann, G. Rumolo, elswhere these proceedings.

[6] T. Raubenheimer et al., Phys. Rev. E **52**, 5487 (1995).

[7] V.V. Danilov, Phys. Rev. ST-Accel. Beams, **1**, 041301, (1998).

[8] H. Fukuma, elswhere these proceedings.

[9] G. Rumolo, F. Zimmermann, elswhere these proceedings.

Appendix A: The Sum of Decrements for a Gaussian Bunch

The sum of eigenvalues is equal to the trace of the mode coupling matrix. Hence, from Eq. (7), the sum of the synchrobetatron mode decrements

$$\sum_{k,l} \text{Im}\,\Omega = -\frac{N r_e c}{2\gamma T_0 \omega_\beta}$$
$$\times \int_{-\infty}^{\infty} d\omega' \text{Re}[Z_1(\omega' + \omega_\xi)] \sum_{k,l} g_{lk}^2(\omega')\,.$$

For a Gaussian bunch, from Eq. (13),

$$2\pi \sum_{k,l} g_{lk}^2(\omega') = e^{-\omega^2\sigma^2/c^2} \sum_{l=-\infty}^{\infty} \sum_{k=0}^{\infty} \frac{(\omega^2\sigma^2/2c^2)^{|l|+2k}}{k!(|l|+k)!}$$
$$= e^{-\omega^2\sigma^2/c^2} \sum_{l=-\infty}^{\infty} I_{|l|}\left(\frac{\omega^2\sigma^2}{c^2}\right)$$
$$= e^{-x}\left(I_0(x) + 2I_1(x) + 2I_2(x) + \ldots\right)$$
$$= e^{-x}e^x = 1\,.$$

Since wakefields are real functions of s, $\text{Re}\,Z_1(\omega)$ is an odd function of ω with a vanishing average. Thus, the sum of the mode decrements, $\sum_{k,l} \text{Im}\,\Omega$, also vanishes.

Appendix B: Effect of Diffusion on Higher-Order Head-Tail Modes

With the fast-oscillating wake (or for a "long" bunch), the positive chromaticity can stabilize all the lower-order head-tail modes up to mode numbers $|l|+2k \leq (\omega_R \sigma_z/c)^2$. However their decrements will be compensated by (small) increments of a large number of higher-order modes to give a vanishing sum. But there is a reason why the higher-order modes are of no special concern.

In e^+e^- machines quantum fluctuations of the synchrotron radiation cause diffusion in particle oscillations. Consider $|l|, k \gg 1$, then the dipole moment is given by the Hermite mode, Eq. (14),

$$\rho_y(z) \propto e^{-z^2/2\sigma^2} H_{|l|+2k}\left(\frac{z}{\sqrt{2}\sigma}\right) \longrightarrow \cos\frac{\tilde{l}z}{\sigma}, \; |z| \leq \sigma.$$

In the above, $\tilde{l} = |l| + 2k$. The Green function of diffusion is

$$G(z,z') = \frac{1}{2\sqrt{\pi Dt}} \exp\left[-\frac{(z-z')^2}{4Dt}\right],$$

where the diffusion constant $D \sim \sigma^2/\tau$, and τ is the radiation damping time.

After a short time, $t \ll \omega_s^{-1}$,

$$\tilde{\rho}_y(z) \sim \int_{-\infty}^{\infty} \rho_y(z')G(z,z')dz'$$
$$\approx \cos\frac{\tilde{l}z}{\sigma} \exp\left[-\frac{\tilde{l}^2 Dt}{\sigma^2}\right] \sim e^{-\tilde{l}^2 t/\tau} \rho_y(z).$$

Thus, while the incoherent damping gives $\tau/\tilde{l}$, the diffusion smear time is even much shorter, $\sim \tau/\tilde{l}^2$.
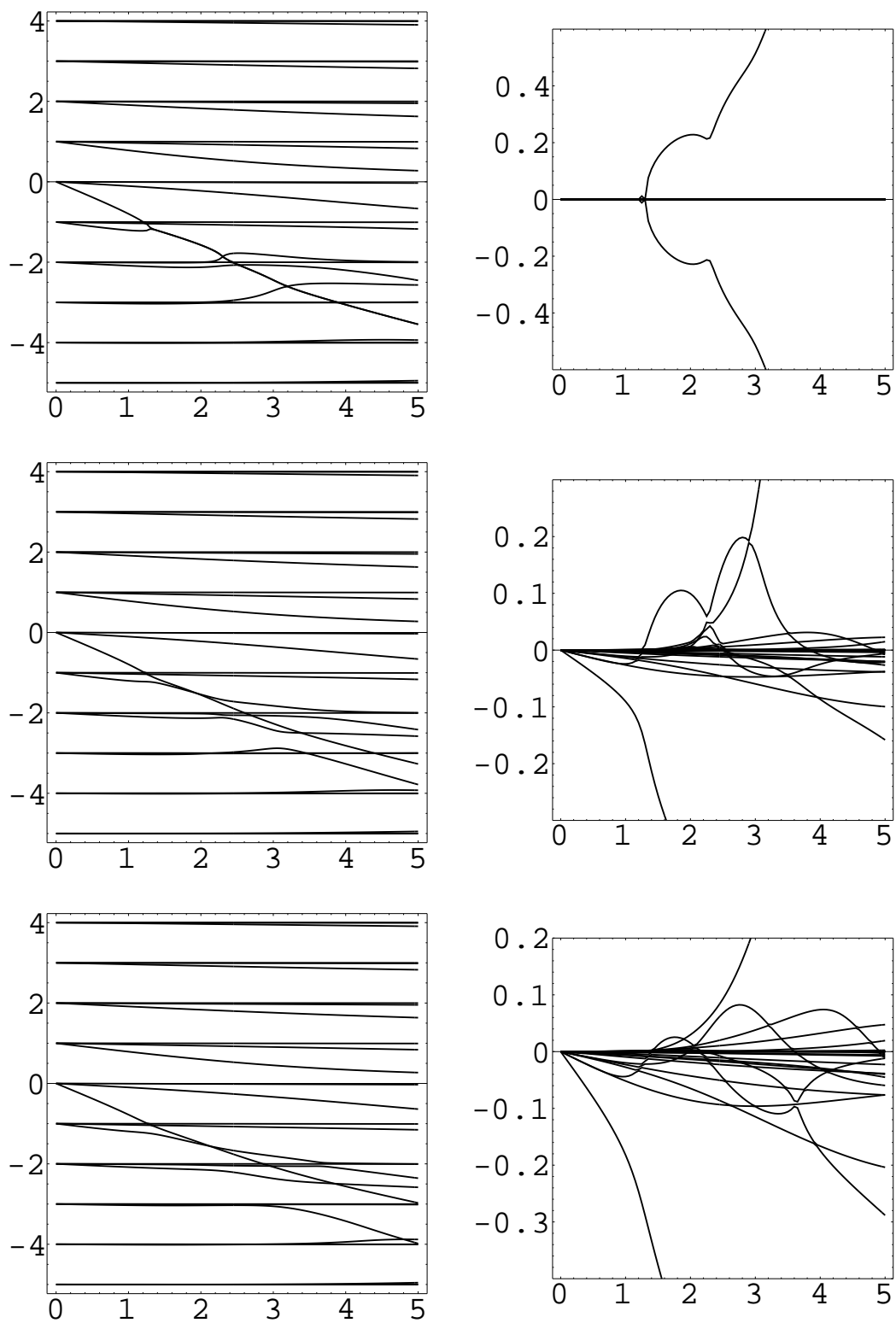
Figure 2: KEKB LER, head-tail mode tunes in units of the synchrotron tune vs the cloud density $\rho_c \times 10^{-12} \mathrm{m}^{-3}$ at $I_b = 0.52 \mathrm{mA}$, $Q = 1$. Left: real part, right: imaginary part. From top to bottom: the chromatic phase is 0.0, 0.25, 0.5.
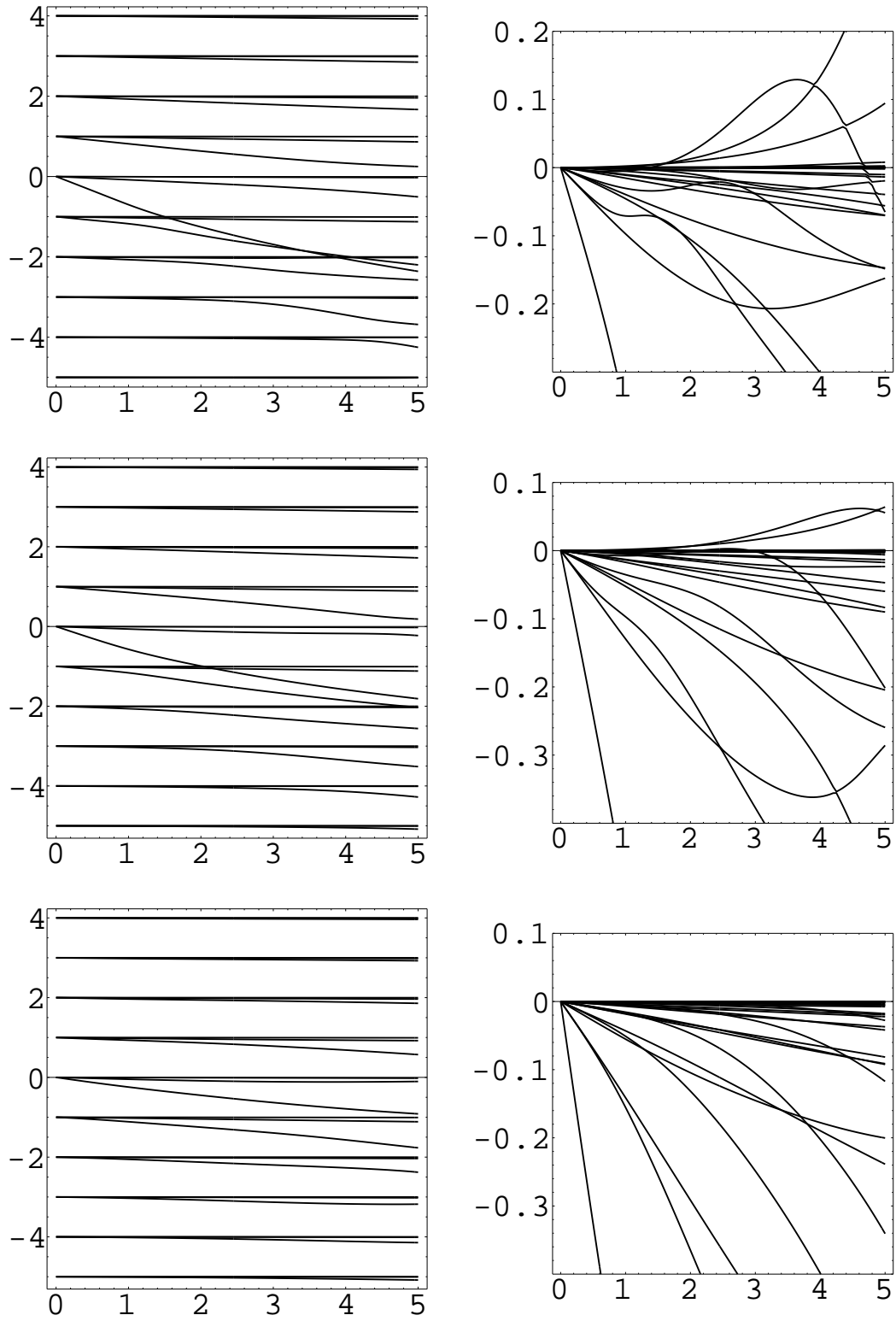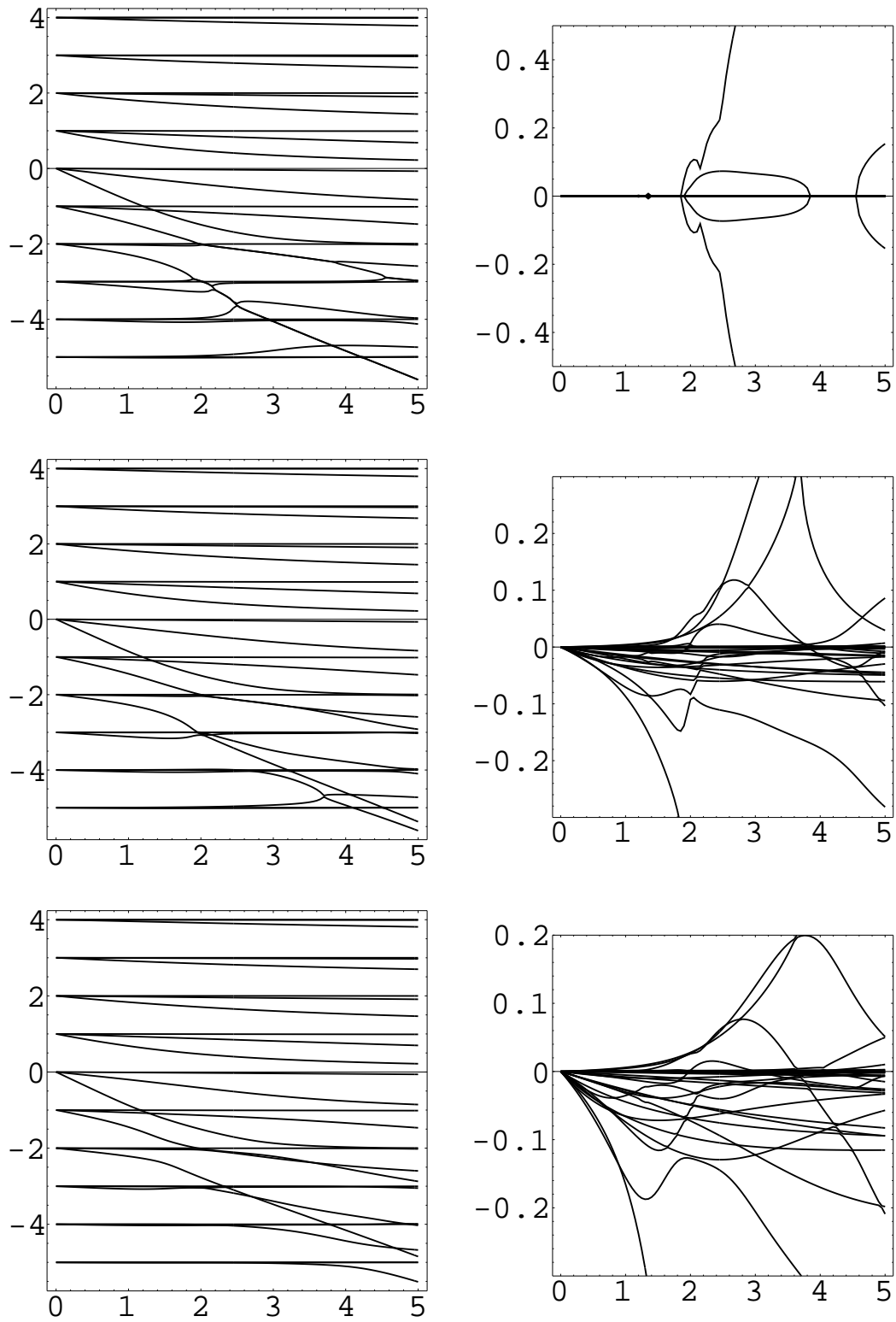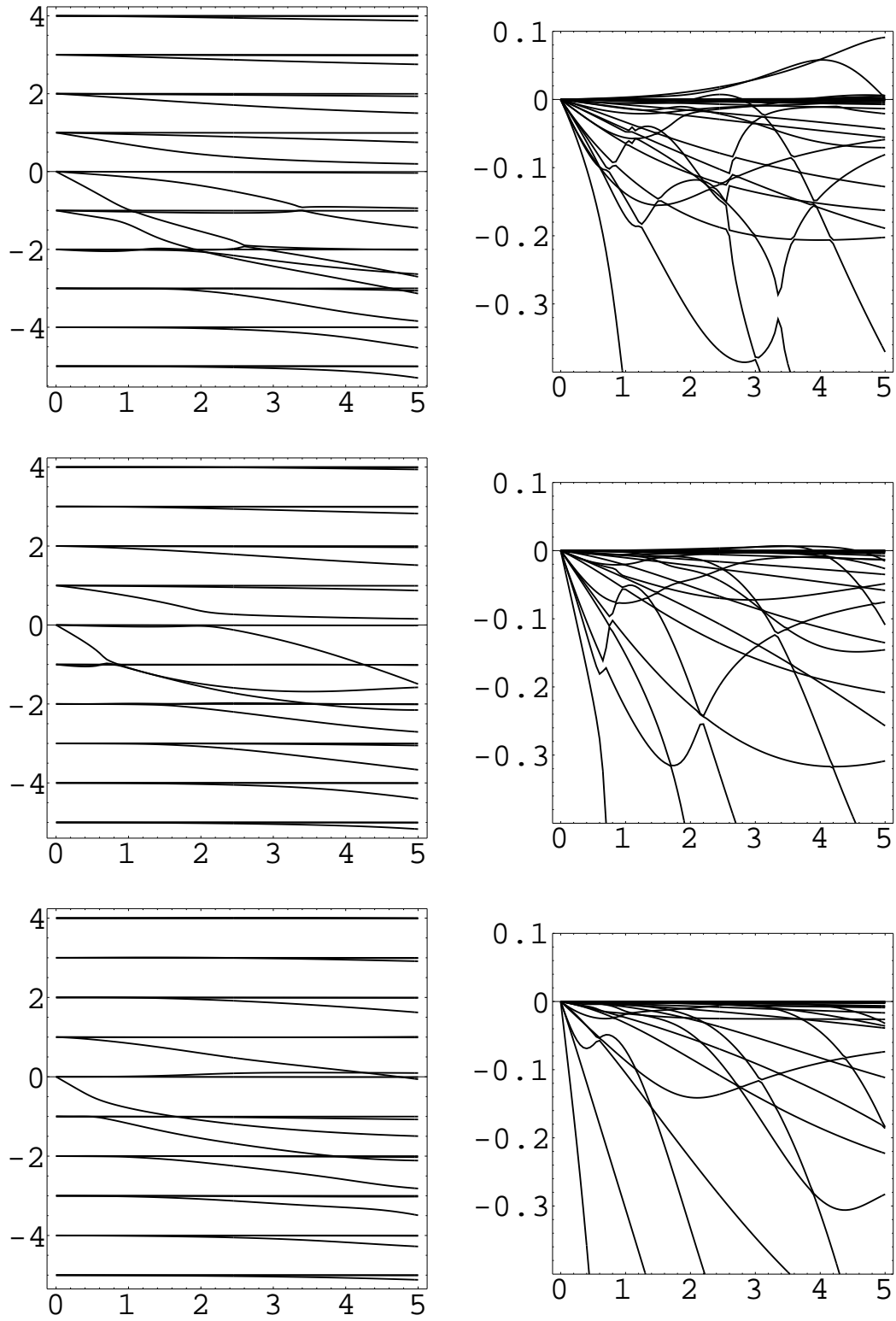
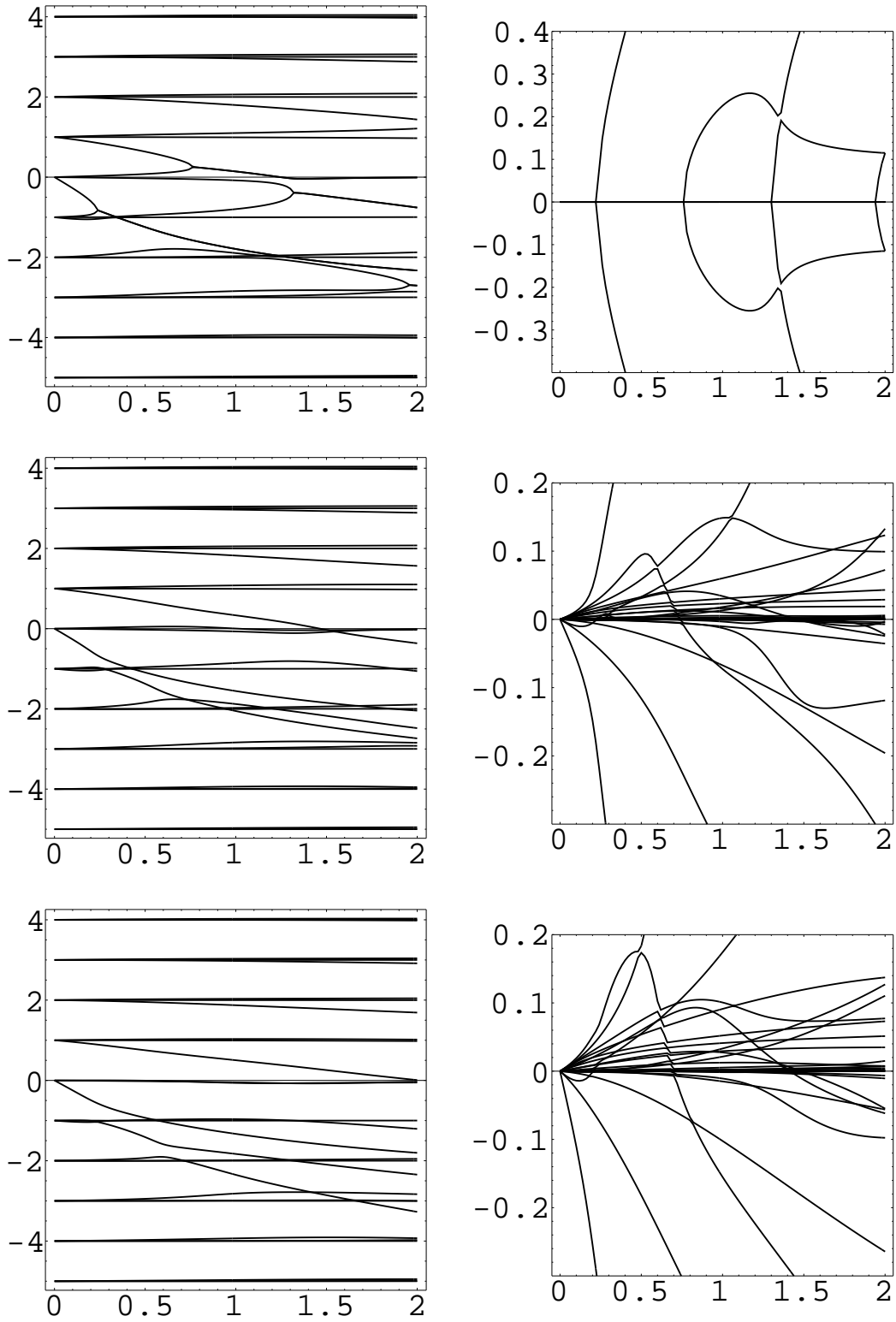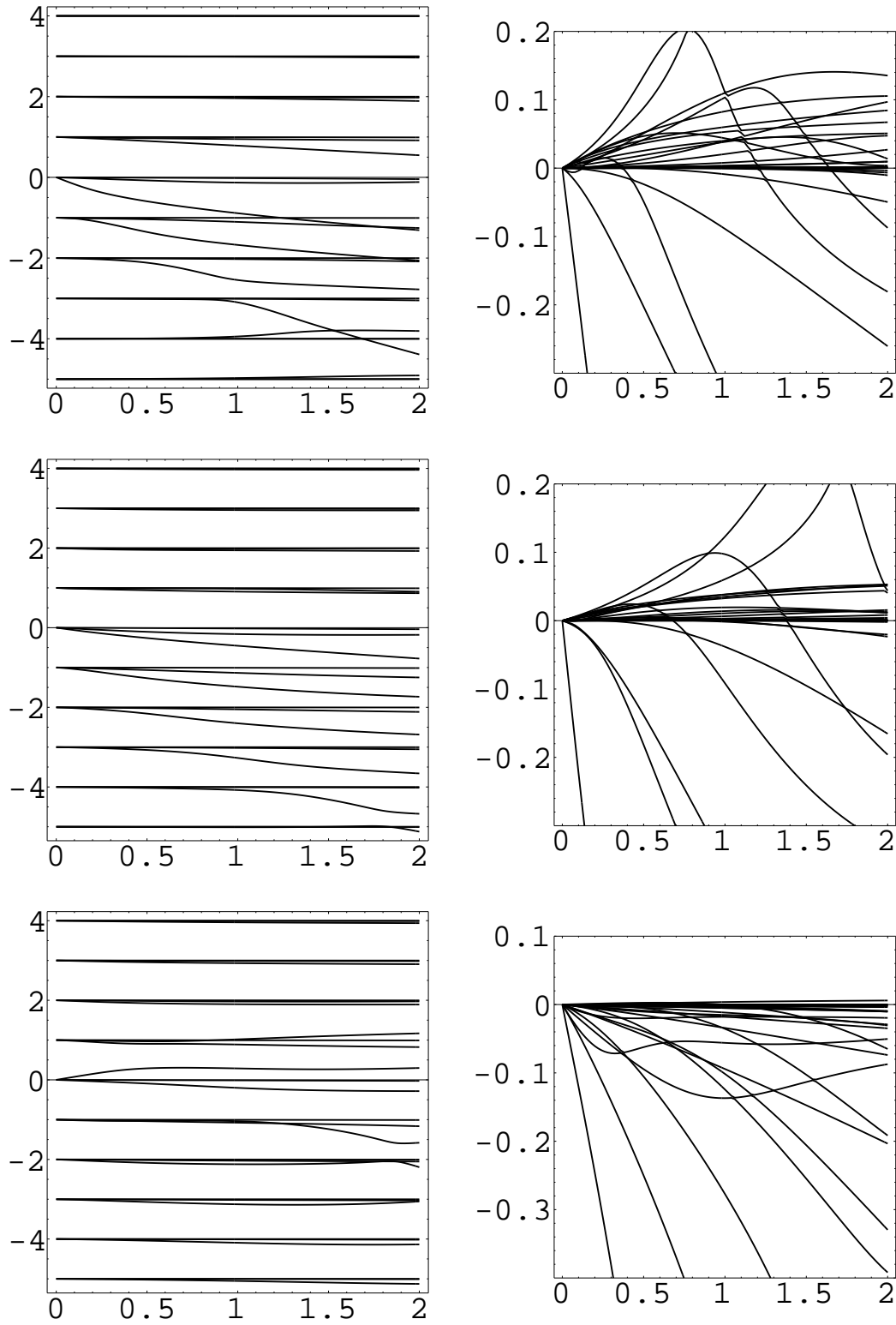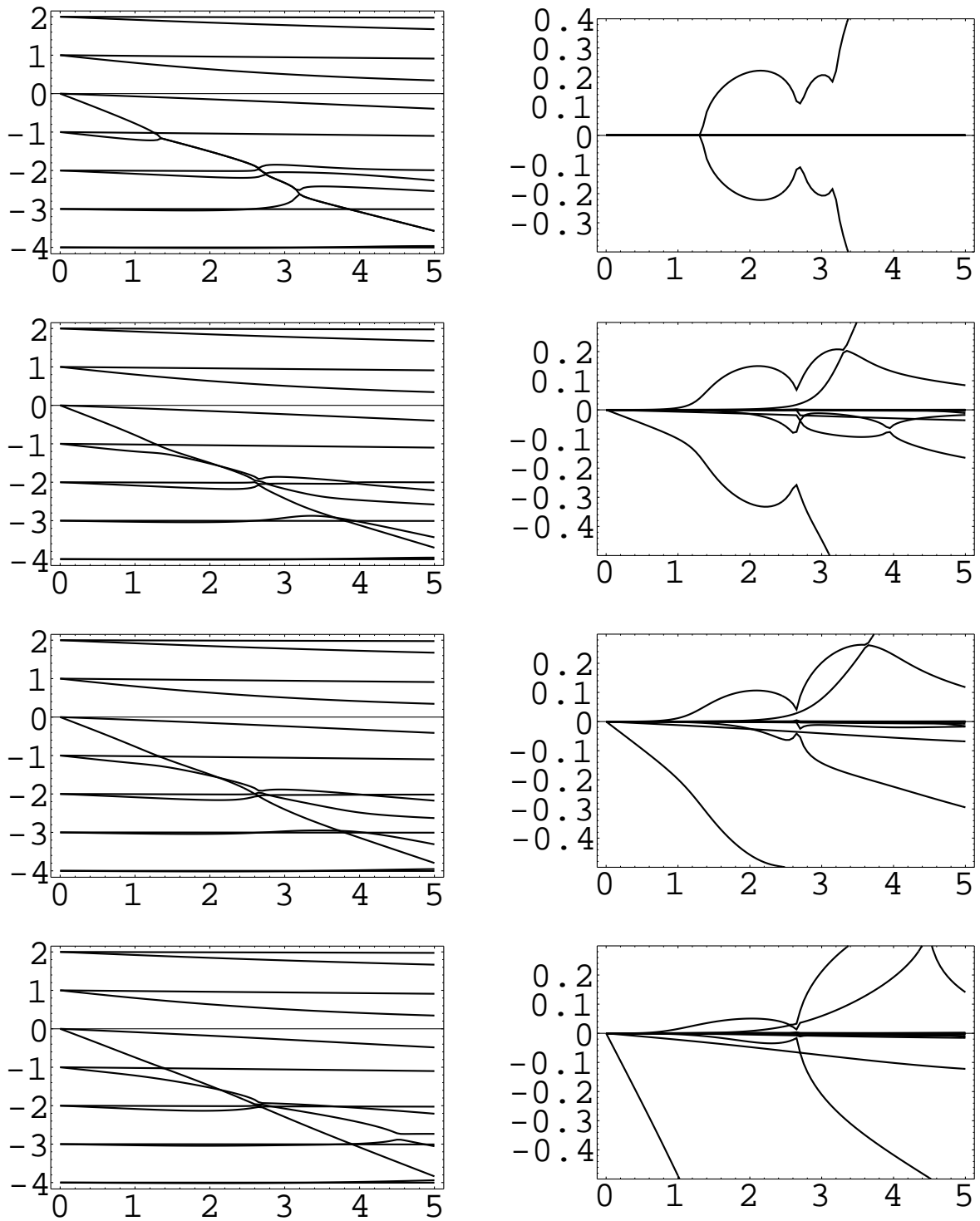Figure 3: Continued from previous figure: KEKB LER, head-tail mode tunes in units of the synchrotron tune vs the cloud density $\rho_c \times 10^{-12} \text{m}^{-3}$ at $I_b = 0.52 \text{mA}$, $Q = 1$. Left: real part, right: imaginary part. From top to bottom: the chromatic phase is 1.0, 1.5, 2.5.
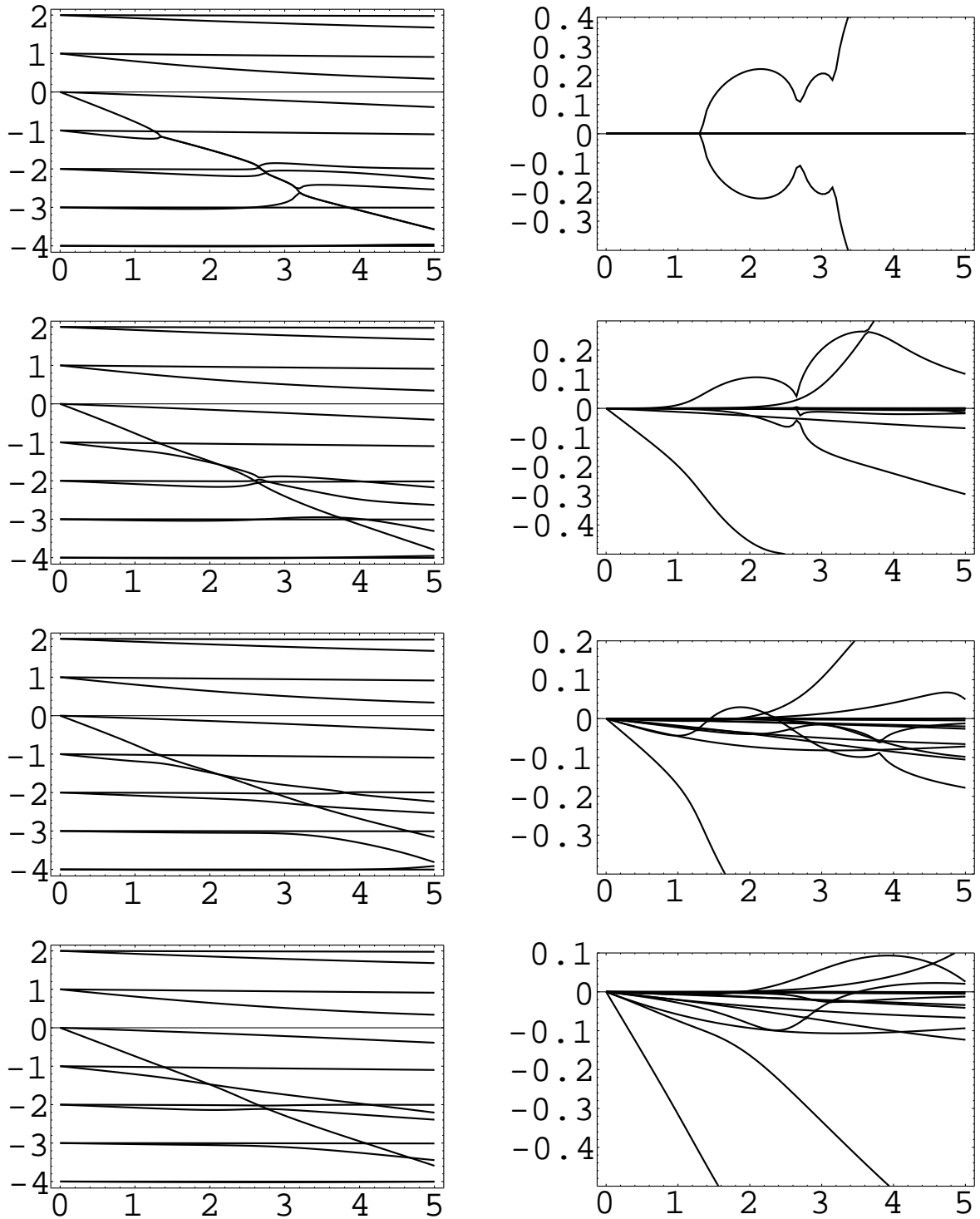
Figure 4: KEKB LER, h ead-tail mode tunes in units of the synchrotron tune vs the cloud density $\rho_c \times 10^{-12} \mathrm{m}^{-3}$ at $I_b = 0.52\mathrm{mA}$, $Q = 6.3$. Left: real part, right: imaginary part. From top to bottom: the chromatic phase is $0.0, 0.25, 0.5$.

Figure 5: Continued from previous figure: KEKB LER, head-tail mode tunes in units of the synchrotron tune vs the cloud density $\rho_c \times 10^{-12} \mathrm{m}^{-3}$ at $I_b = 0.52\mathrm{mA}$, $Q = 6.3$. Left: real part, right: imaginary part. From top to bottom: the chromatic phase is 1.0, 1.5, 2.0.

Figure 6: CERN SPS, head-tail mode tunes in units of the synchrotron tune vs the cloud density $\rho_c \times 10^{-12} \text{m}^{-3}$ at $N_b = 10^{11}$, $Q = 2$. Left: real part, right: imaginary part. From top to bottom: the chromatic phase is 0.0, 0.25, 0.5.

Figure 7: Continued from previous figure: CERN SPS, head-tail mode tunes in units of the synchrotron tune vs the cloud density $\rho_c \times 10^{-12} \mathrm{m}^{-3}$ at $N_b = 10^{11}$, $Q = 2$. Left: real part, right: imaginary part. From top to bottom: the chromatic phase is 1.0, 1.5, 2.5.
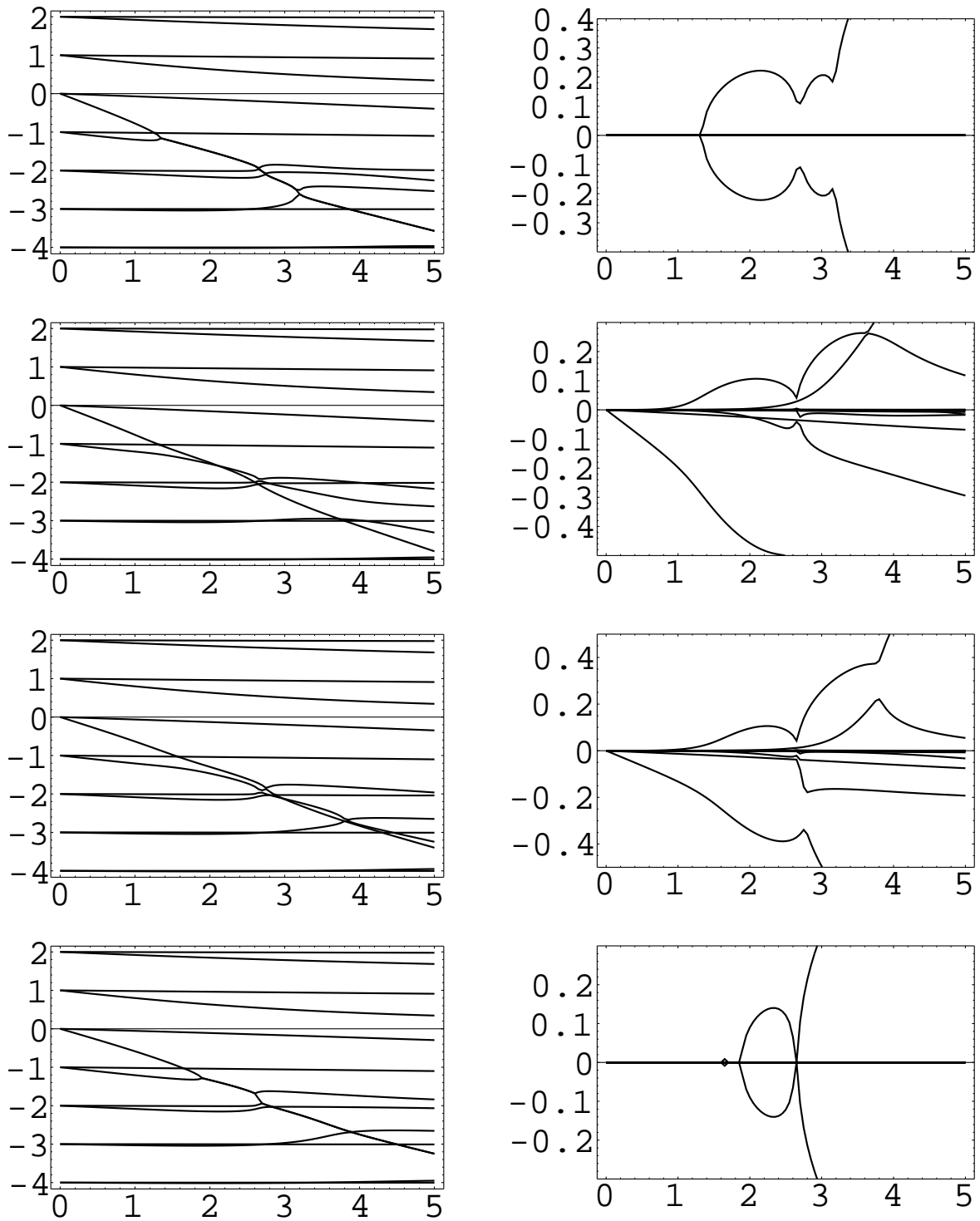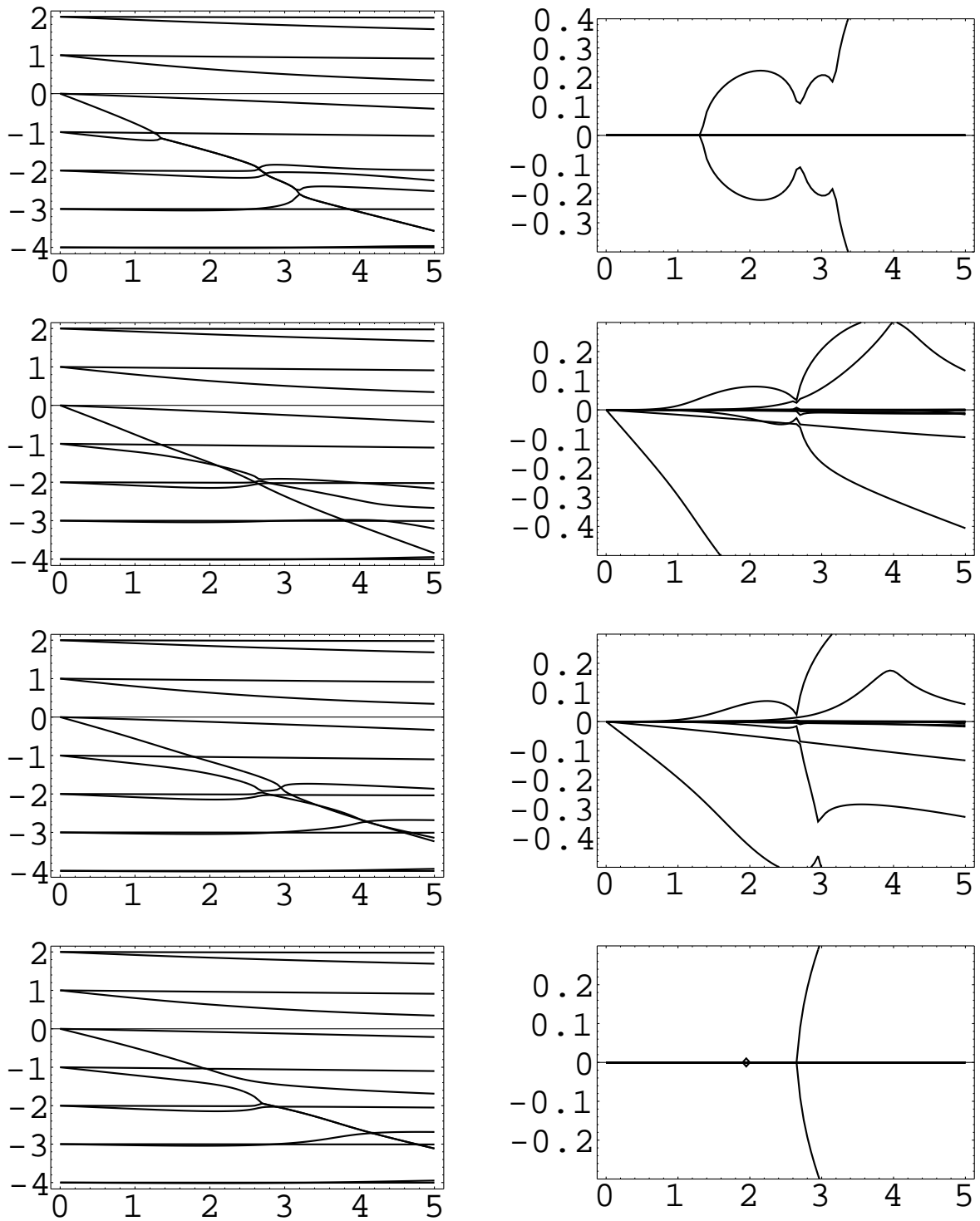
Figure 8: KEKB LER, head-tail mode tunes in units of the synchrotron tune vs the cloud density $\rho_c \times 10^{-12} \text{m}^{-3}$. Left: real part, right: imaginary part. From top to bottom: the feedback damping is 0.0, 0.1, 0.2, 0.5; $Q = 1$, $I_b = 0.52 \text{mA}$ and zero chromaticity.

Figure 9: KEKB LER, head-tail mode tunes in units of the synchrotron tune vs the cloud density $\rho_c \times 10^{-12} \mathrm{m}^{-3}$. Left: real part, right: imaginary part. Combined action of the chromaticity and feedback, from top to bottom: a) no feedback, no chromaticity; b) the feedback damping is 0.2; c) no feedback and the chromatic phase is 0.5; d) the feedback damping is 0.2, and the chromatic phase is 0.5. $Q = 1$, $I_b = 0.52 \mathrm{mA}$.
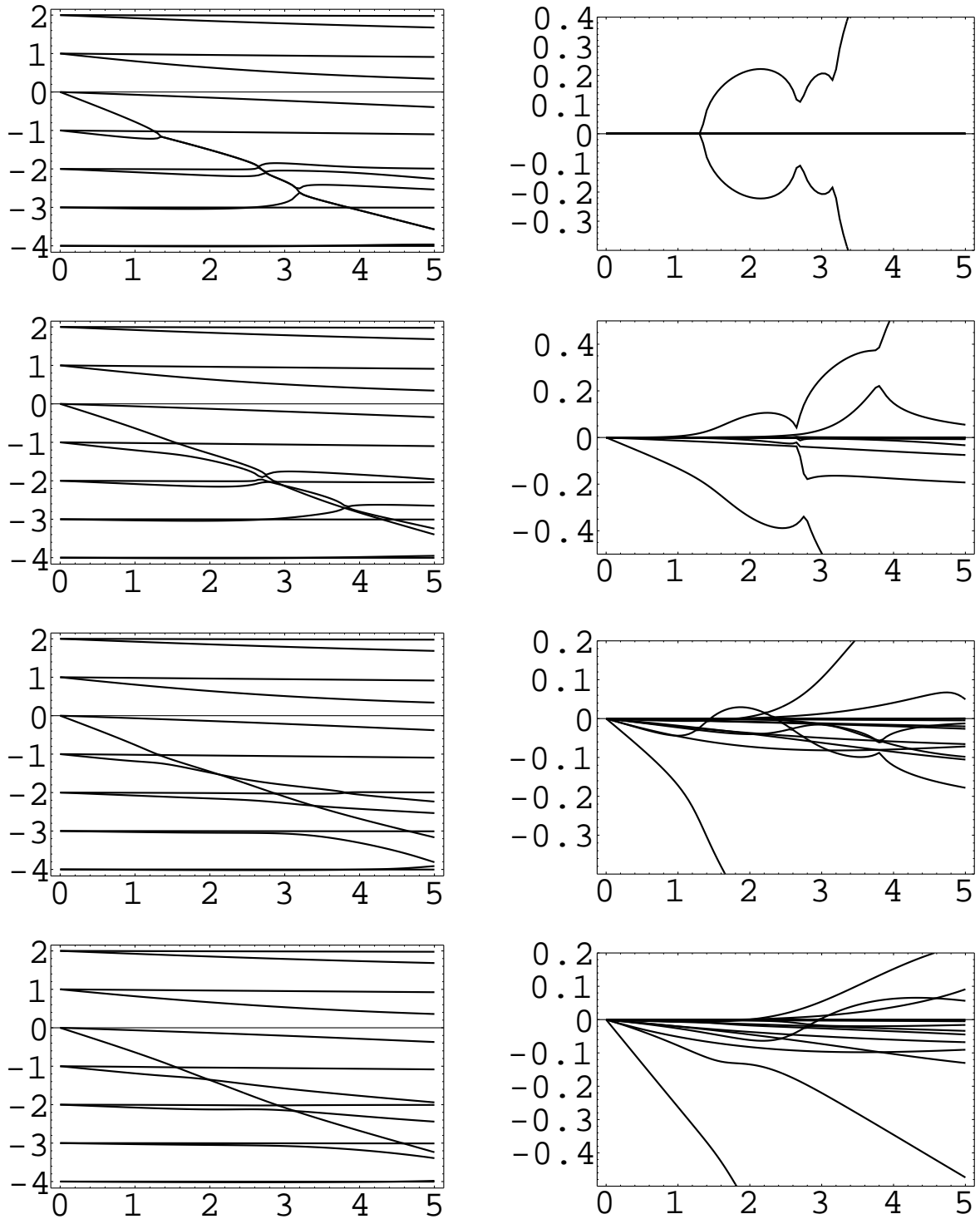
Figure 10: KEKB LER, head-tail mode tunes in units of the synchrotron tune vs the cloud density $\rho_c \times 10^{-12} \mathrm{m}^{-3}$. Left: real part, right: imaginary part. Effect of the feedback phase, from top to bottom: a) no feedback; b-d) the feedback damping is 0.2, and its phase is varied 90°, 135°, 180°. $Q = 1$, $I_b = 0.52$mA.

Figure 11: KEKB LER, head-tail mode tunes in units of the synchrotron tune vs the cloud density $\rho_c \times 10^{-12}$m^{-3}. Left: real part, right: imaginary part. Effect of the feedback phase, from top to bottom: a) no feedback; b-d) the feedback damping is 0.3, and its phase is varied 90°, 135°, 180°. $Q = 1$, $I_b = 0.52$mA.

Figure 12: KEKB LER, head-tail mode tunes in units of the synchrotron tune vs the cloud density $\rho_c \times 10^{-12}\text{m}^{-3}$. Left: real part, right: imaginary part. Combined action of the chromaticity and feedback, from top to bottom: a) no feedback, no chromaticity; b) the feedback damping is 0.2, its phase is 135°; c) no feedback, the chromatic phase is 0.5; d) the feedback damping is 0.2, its phase is 135° and the chromatic phase is 0.5. $Q = 1$, $I_b = 0.52\text{mA}$.
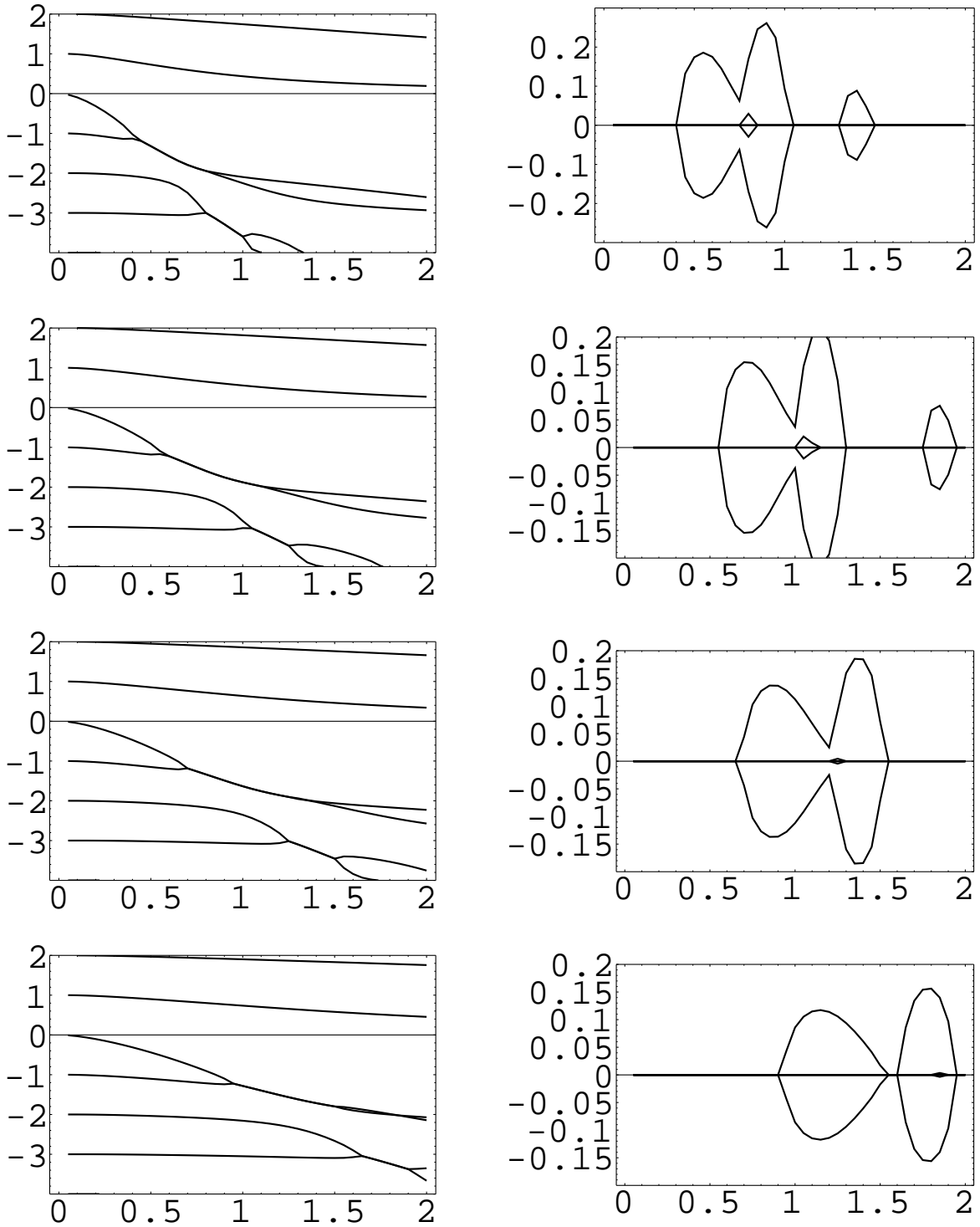
Figure 13: KEKB LER, head-tail mode tunes in units of the synchrotron tune vs the bunch current, mA. Left: real part, right: imaginary part. From top to bottom: the bunch spacing is 2, 3, 4, 6; $Q = 1$.
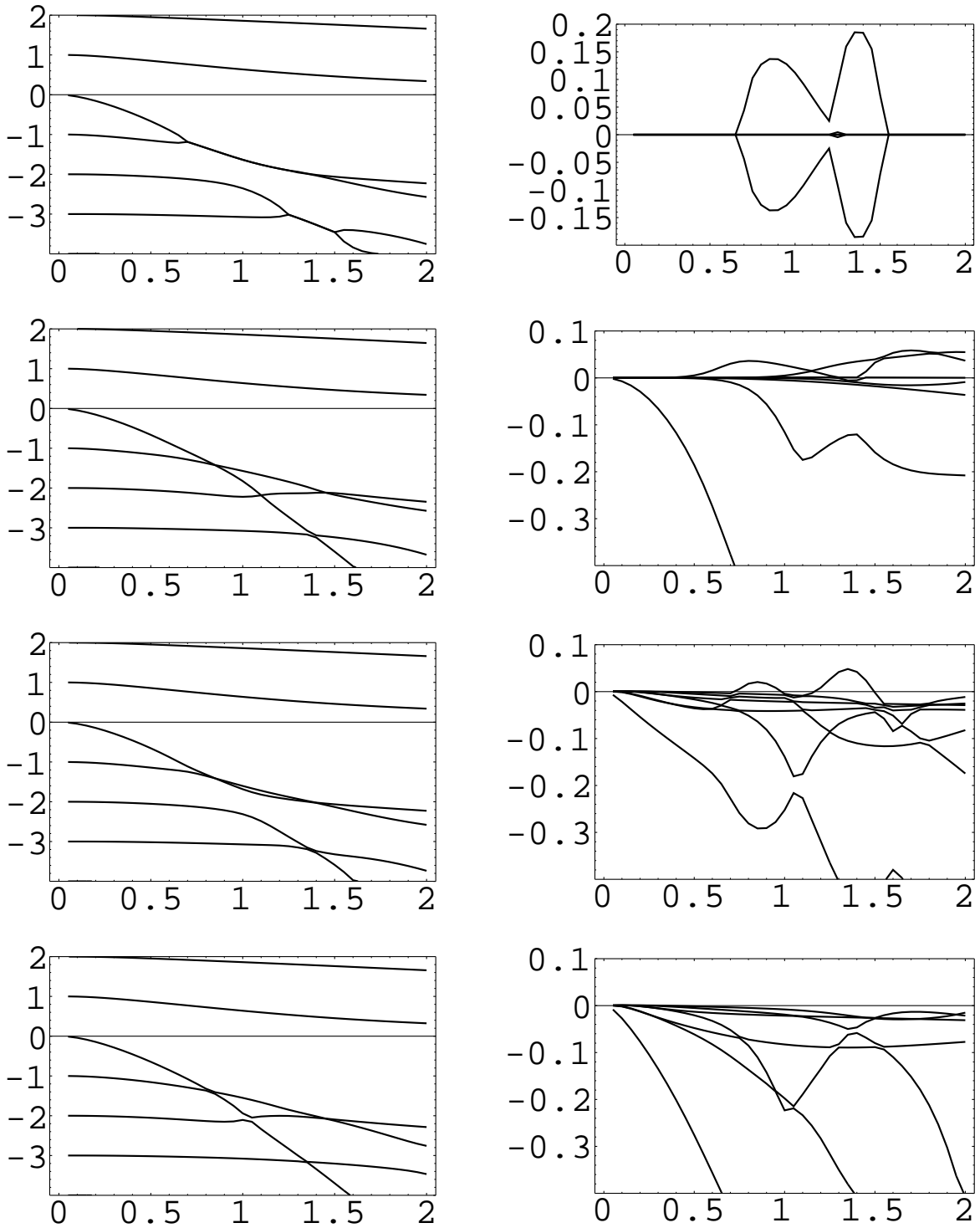
Figure 14: KEKB LER, head-tail mode tunes in units of the synchrotron tune vs the bunch current, mA. Left: real part, right: imaginary part. Combined action of the chromaticity and feedback, from top to bottom: a) no feedback, no chromaticity; b) the feedback damping is 0.2; c) no feedback and the chromatic phase is 0.5; d) the feedback damping is 0.2, and the chromatic phase is 0.5. $Q = 1$.
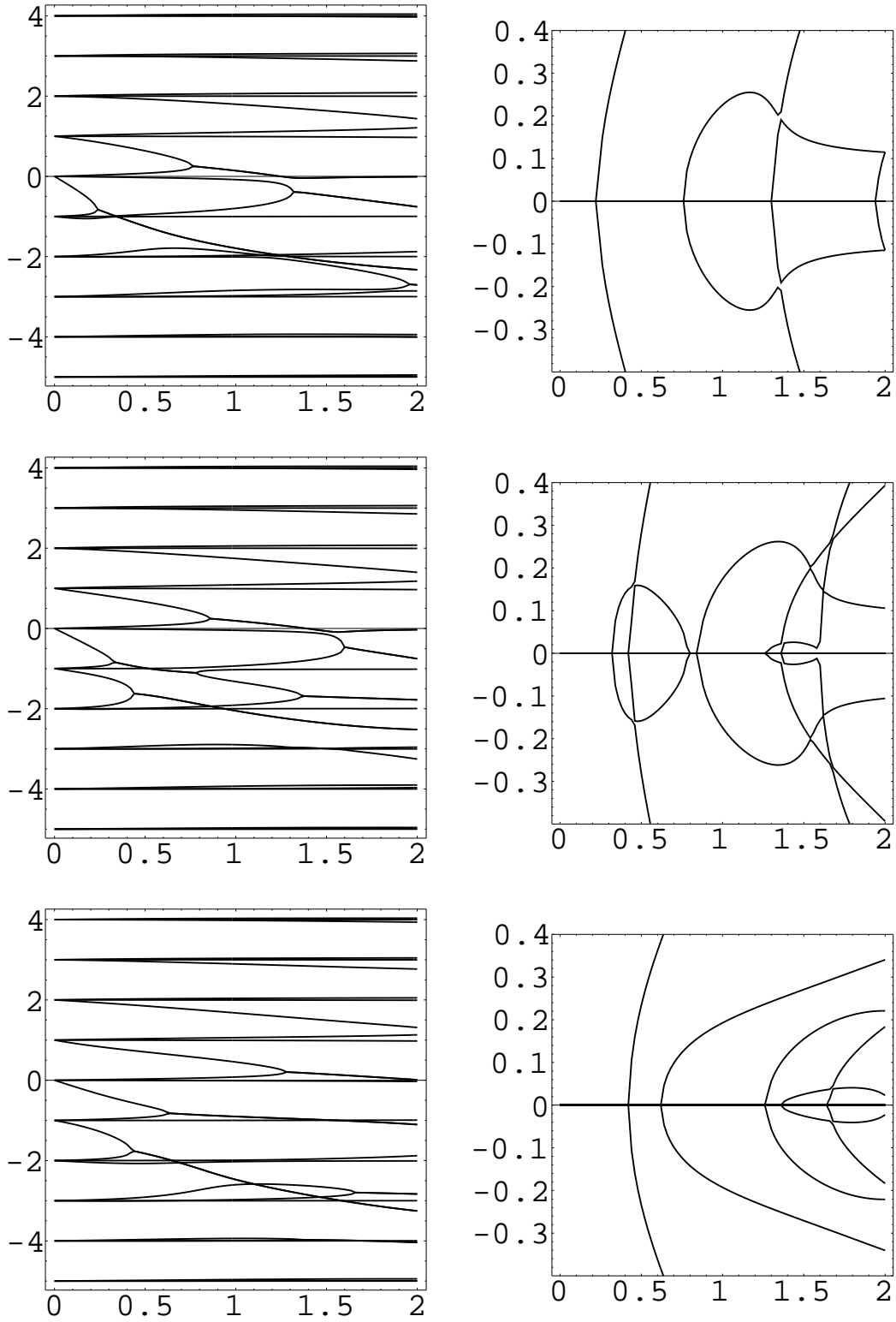
Figure 15: CERN SPS, head-tail mode tunes in units of the synchrotron tune vs the cloud density $\rho_c \times 10^{-12} \mathrm{m}^{-3}$ at $N_b = 10^{11}$, $Q = 2$, zero chromaticity, at different tune variation. Left: real part, right: imaginary part. From top to bottom: the tune variation is 0.0, 0.5, 1.0.
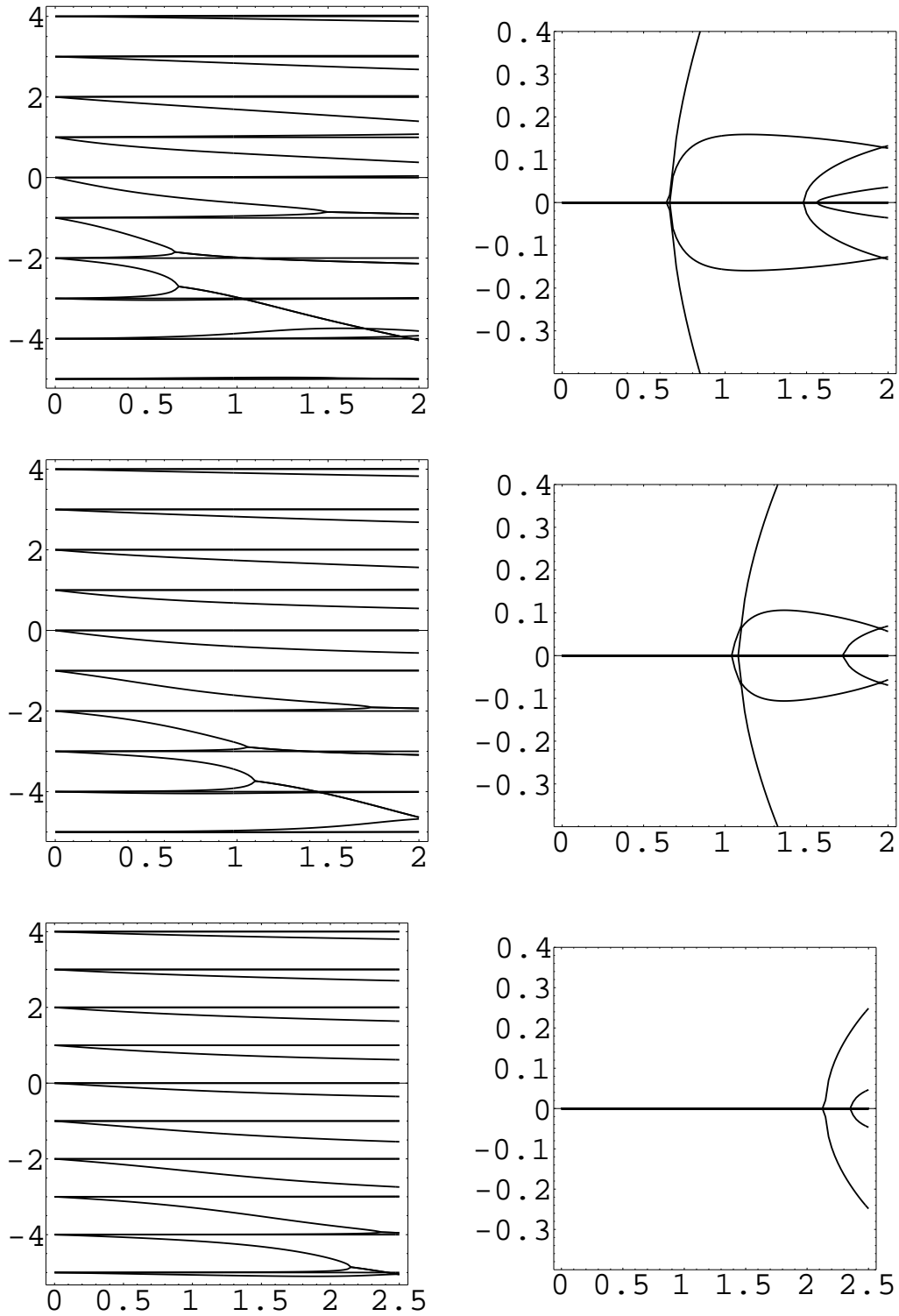
Figure 16: Continued from previous figure: CERN SPS, head-tail mode tunes in units of the synchrotron tune vs the cloud density $\rho_c \times 10^{-12} \text{m}^{-3}$ at $N_b = 10^{11}$, $Q = 2$, zero chromaticity, at different tune variation. Left: real part, right: imaginary part. From top to bottom: the tune variation is 1.5, 2.0, 2.5.
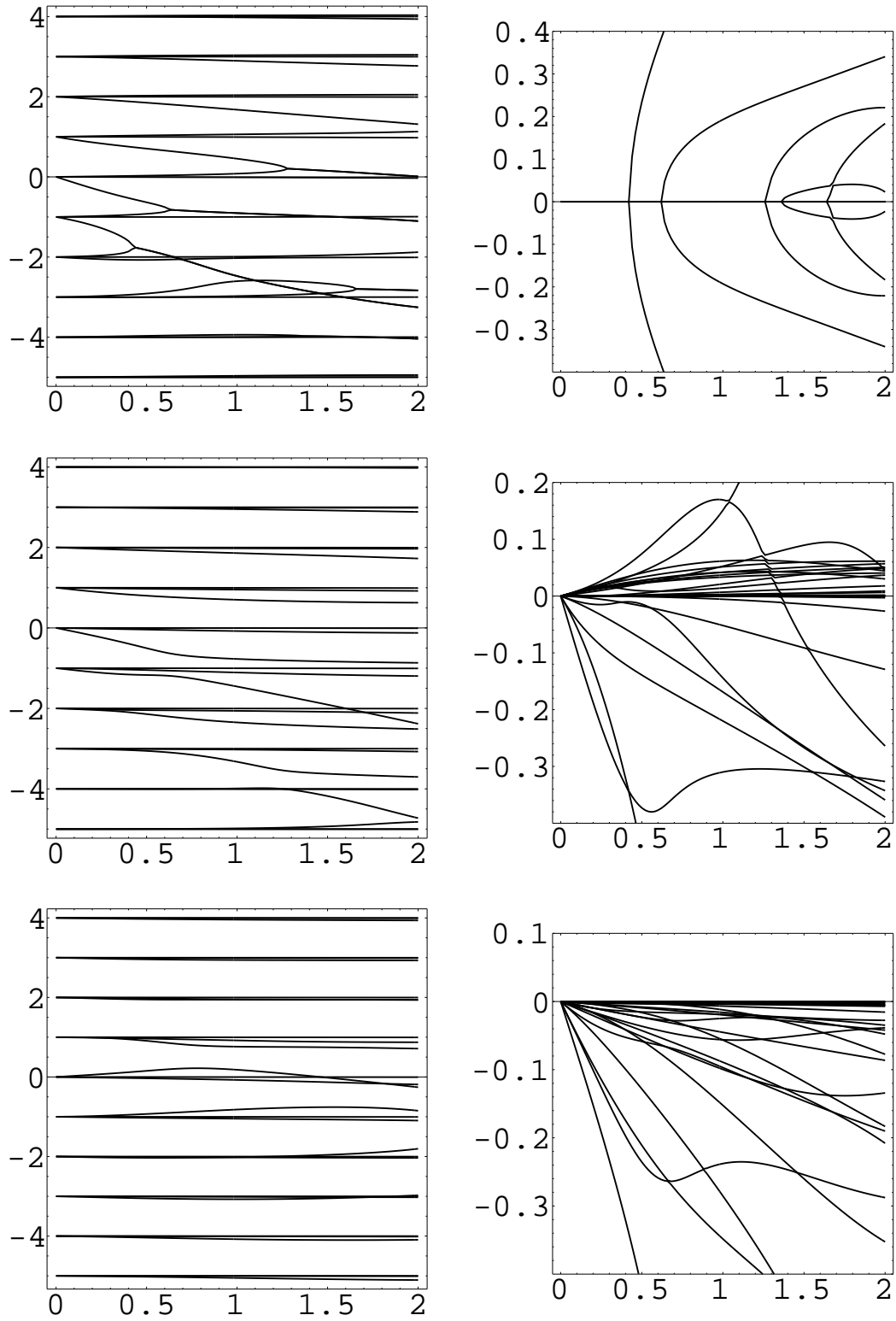
Figure 17: CERN SPS, head-tail mode tunes in units of the synchrotron tune vs the cloud density $\rho_c \times 10^{-12}\text{m}^{-3}$ at $N_b = 10^{11}$, $Q = 2$, the tune variation is 1.0. Left: real part, right: imaginary part. From top to bottom: the chromatic phase is 0.0, 1.0, 2.5.